

**Phenotypic Rescue of a Nonsense Mutation in TRAPPC11 using Translational Read-
through Inducing Drugs**

Kaylyn Chase

A Thesis

In the Department

Of

Biology

Presented in Partial Fulfillment of the
Requirements for the Degree of Master of Science
(Biology) at Concordia University
Montréal, Quebec, Canada

March 2022

© Kaylyn Chase, 2022

CONCORDIA UNIVERSITY
School of Graduate Studies

This is to certify that the thesis

Prepared by: Kaylyn Chase
Entitled: Phenotypic Rescue of a Nonsense Mutation in TRAPPC11 using
Translational Read-through Inducing Drugs

and submitted in partial fulfillment of the requirements for the degree of

Master of Science (Biology)

complies with the regulations of the University and meets the accepted standards with respect to originality and quality.

Signed by the final Examining Committee:

_____	Chair
Chair's Name	
_____	Examiner
Dr. Alisa Piekny	
_____	Examiner
Dr. William Zerges	
_____	External Examiner
Dr. Brandon Helfield	
_____	Supervisor
Dr. Michael Sacher	

Approved by

Dr. Robert Weladji, Graduate Program Director

Dr. Pascale Sicotte, Dean of Faculty of Arts and Sciences

_____ 2022

Abstract

Phenotypic Rescue of a Nonsense Mutation in TRAPPC11 using Translational Read-through

Inducing Drugs

Kaylyn Chase, MSc

The TRAPP family of complexes are multisubunit tethering complexes that function in membrane trafficking. There are two TRAPP complexes that have been identified in humans: TRAPP II and TRAPP III. TrappC11 is a protein found in the TRAPP III complex and has been demonstrated to play a role in membrane trafficking, autophagy, glycosylation, and Golgi morphology. Individuals with mutations in this gene display phenotypes including developmental delay, epilepsy, cerebral atrophy, muscular dystrophy, skeletal abnormalities, and hepatomegaly. Drug induced read-through of nonsense codons could be a method of treating individuals with nonsense mutations in TRAPPC11 that result in a nonsense codon. Translational read-through inducing drugs (TRIDs) are small molecule drugs, such as Ataluren and Amlexanox, that function to suppress nonsense codons. This project aims to study the potential read-through efficacy of Ataluren and Amlexanox on fibroblasts derived from an individual with a compound heterozygous mutation where one allele has a nonsense mutation. The other TRAPPC11 patient presented in this paper is used as a comparison, as this patient does not have a nonsense mutation and therefore should not benefit from treatment with TRIDs. Results show treatment with Ataluren or Amlexanox improves various cellular functions in the patient with a nonsense mutation. It is noteworthy that Ataluren is approved for use in the UK and Amlexanox was used in the past in the USA for other human conditions. Further work aims to build upon the preliminary results observed thus far.

Acknowledgements

I would like to begin by thanking my supervisor, Dr. Michael Sacher, for your endless support, exceptional teaching, constructional advice, and continuous encouragement throughout the past few years. I have learned and grown during my time with you more than I ever thought possible.

To my fellow labmates: thank you to each one of you! I have learned an invaluable amount from you all. Your friendship and endless support has been tremendous.

To my friends in Montréal: you have made this an unforgettable time in my life. Thank you for your love and support.

To my entire family, thank you for everything. Thank you for giving me the confidence I needed to leave California and pursue a degree in Montréal. Thank you especially to my dad, Brian. I could not have done this without your unconditional love, support, advice, and fatherly mentorship. You mean the world to me.

Most importantly, this is dedicated to my mom, Theresa.

Contribution of Authors

Figure 3.5 - Hashem Almousa did the neon transfection of the fibroblasts and did the microscopy for the RUSH assay. I completed the quantifications with ImageJ.

Table of Contents

<i>List of Figures</i>	<i>viii</i>
<i>List of Tables</i>	<i>ix</i>
<i>List of Abbreviations</i>	<i>x</i>
1. Introduction	1
1.1 Membrane Trafficking	1
1.2 TRAPP Complexes	2
Figure 1.1. A schematic representation of TRAPP II and TRAPP III mammalian complexes	3
1.3 TRAPPC11 Mutations in Human Diseases	4
Figure 1.2. A schematic of the TRAPPC11 protein and known mutations.....	5
1.4 Autophagy	6
Figure 1.3. A representation of the TRAPP III proteins in autophagy.	8
1.5 Nonsense mutations	8
Figure 1.4. A representation of normal protein translation in comparison to translation that is hindered due to a nonsense mutation	9
1.6 Translational Read-through Inducing Drugs (TRIDs)	10
1.7 Objective	12
2. MATERIALS AND METHODS	13
2.1 Cell Culture	13
2.2 Starvation Treatments	13
2.3 Translational Read-Through Drugs (TRIDs)	13
2.4 Antibodies and Dyes	14
2.5 Immunofluorescence microscopy	14
2.6 Western blotting	15
2.7 Retention using selective hooks (RUSH) assay	15
2.8 DNA constructs	16
3. RESULTS	18
3.1 Clinical summary of TRAPPC11 individuals B18 and B19	18
Table 3.1. Summary of clinical phenotypes in three TRAPPC11 patients	21
3.2 Cryo-EM structure of TRAPPC11 and location of mutations	21
Figure 3.1 Cryo-EM structure of TRAPP III.....	22
3.3 Autophagy protein LC3-II is elevated in TRAPPC11 individual B18, but not in B1922 Figure 3.2. An autophagy defect in cells from individual B18 can be rescued by TRIDs	24

3.4 TRID treatment rescues the autophagic defect in TRAPPC11 B18 cells, but not in B19 cells.....	25
3.5 Number of Golgi fragments per cell in B18 cells decreased with TRID treatment	26
Figure	28
3.6 Ataluren rescues membrane trafficking defect in B18 fibroblasts.....	28
Figure 3.4. Trafficking from ER to the Golgi is defective in B18 fibroblasts and rescued after treatment with Ataluren.....	31
3.7 TRIDs do not induce observable read-through in transfected HeLa cells	31
Figure 3.5. HeLa cells transfected with TRAPPC11 reporter construct do not appear to show TRID-induced read-through of the nonsense codon	32
4. DISCUSSION.....	33
Figure 4.1. Four models of Golgi fragmentation.....	36
<i>Citations</i>.....	40

List of Figures

Figure 1.1. A schematic representation of TRAPP II and TRAPP III mammalian complexes	3
Figure 1.2. A schematic of the TRAPPC11 protein and known mutations	5
Figure 1.3. A representation of the TRAPP III proteins in autophagy	8
Figure 1.4. A representation of normal protein translation in comparison to translation that is hindered due to a nonsense mutation	9
Table 3.1. Summary of clinical phenotypes in three TRAPPC11 patients	21
Figure 3.1 Cryo-EM structure of TRAPP III	22
Figure 3.2. An autophagy defect in cells from individual B18 can be rescued by TRIDs	24
Figure	28
Figure 3.4. Trafficking from ER to the Golgi is defective in B18 fibroblasts and rescued after treatment with Ataluren	31
Figure 3.5. HeLa cells transfected with TRAPPC11 reporter construct do not appear to show TRID-induced read-through of the nonsense codon	32
Figure 4.1. Four models of Golgi fragmentation	36

List of Tables

Table 3.1: Summary of clinical phenotypes in three TRAPPC11 patients	18
--	----

List of Abbreviations

TRAPP	Transport protein particle
TRIDs	Translational read-through inducing drugs
Ata	Ataluren
Aml	Amlexanox
ER	Endoplasmic reticulum
TGN	Trans-Golgi network
SNARE	Soluble N-ethylmaleimide sensitive attachment protein receptor
Cryo-EM	Cryogenic electron microscopy
LC3-I/LC3-II	Microtubule-associated protein 1A/1B-light chain 3
mRNA	messenger RNA
tRNA	transfer RNA
eRF1/eRF3	Eukaryotic release factor 1 and 3
NMD	Nonsense mediated mRNA decay
PTC124	Alternate name for Ataluren

1. Introduction

1.1 Membrane Trafficking

Membrane trafficking is an essential cellular process that ensures proteins of the endomembrane system are properly sorted and sent to the correct location within a cell (Palade, 1975). Two intracellular compartments that have major roles in this process include the endoplasmic reticulum (ER) and the Golgi apparatus. Trafficking within the endomembrane system begins at the ER, continues through the Golgi apparatus, and ends at either a different organelle (e.g. lysosome), the plasma membrane or the protein is secreted (Howell et al., 2006). Retrograde transport balances the forward (anterograde) movement of the pathway by working to shuttle proteins in the opposite direction. The two opposing pathways work together to maintain cellular homeostasis (Antonescu et al., 2014).

The highly complex process of membrane trafficking can be reduced to four main steps: 1) vesicle budding from a donor membrane, 2) vesicle transport, 3) vesicle tethering and 4) vesicle fusion to an acceptor membrane (Bonifacino & Glick, 2004). Each of these steps are carefully regulated to ensure proper protein sorting and transport. To begin, vesicle budding from the donor membrane involves the deformation of the flat membrane surface (Bi et al., 2002). The deformation of this surface is aided by coat proteins that interact with cargo protein components that were selected for trafficking (Bröcker et al., 2010), thus forming a spherical vesicle that pinches off from the donor membrane (Bonifacino & Lippincott-Schwartz, 2003).

Three coat protein complexes that are crucial for vesicle budding are clathrin, COP-I and COP-II. Clathrin proteins facilitate budding and transport between the *trans*-Golgi Network (TGN)

and either the plasma membrane or endosomes (Pearse, 1976). ER-to-Golgi trafficking involves COP-I and COP-II protein complexes. COP-II proteins facilitate vesicle budding and transport in the early part of the anterograde pathway from the ER to the Golgi (Barlowe, 1994). COP-I proteins function complementary to COP-II proteins, by mediating budding from the Golgi and transport to the ER (Letourneur et al., 1994; Stephens et al., 2000).

After budding from the donor membrane, the protein coated vesicle is targeted to a specific membrane. The movement of the vesicle between the ER and Golgi is mediated by a cytoskeletal network of microtubules (Klann et al., 2012). Once the vesicle nears its destination, tethering and the initiation of fusion occur. Tethering to and fusion with the acceptor membrane are mediated by the interaction between tethering proteins and SNARE (soluble *N*-ethylmaleimide sensitive attachment protein receptor) proteins. Tethering proteins can be divided into two groups: coiled-coil proteins and multimeric complexes (Cai et al., 2008). Multisubunit tethering complexes that are well characterized in yeast and humans are the Transport Protein Particle (TRAPP) family of complexes (Kim et al., 2016). SNARE proteins are thought to provide the energy in the process of fusion (Nichols et al., 1997). These proteins form a complex and pull the vesicle and the target membrane together, facilitating fusion (Fasshauer et al., 1998; Sutton et al., 1998). The tightly regulated steps of budding, transport, tethering and fusion are key to ensure proper membrane trafficking events.

1.2 TRAPP Complexes

The TRAPP family of complexes were first identified in yeast, and have since been identified in metazoans (Rossi et al., 1995; Sacher, 1998; Sacher et al., 2000). In yeast, there were initially

three TRAPP complexes reported: TRAPP I, TRAPP II and TRAPP III. However, more recently the TRAPP I complex was suggested to be an artifact and not seen in vivo (Brunet et al., 2012; Thomas et al., 2018). Accordingly, in humans only TRAPP II and TRAPP III have been identified (Bassik et al., 2013; Zhao et al., 2017). The two different TRAPP complexes are each composed of a common core of 7 distinct proteins: TRAPPC1, TRAPPC2, TRAPPC2L, two copies of TRAPPC3, TRAPPC4, TRAPPC5 and TRAPPC6. Along with the core of proteins, TRAPP II contains TRAPPC9 and TRAPPC10, while TRAPP III contains TRAPPC8, TRAPPC11, TRAPPC12 and TRAPPC13.

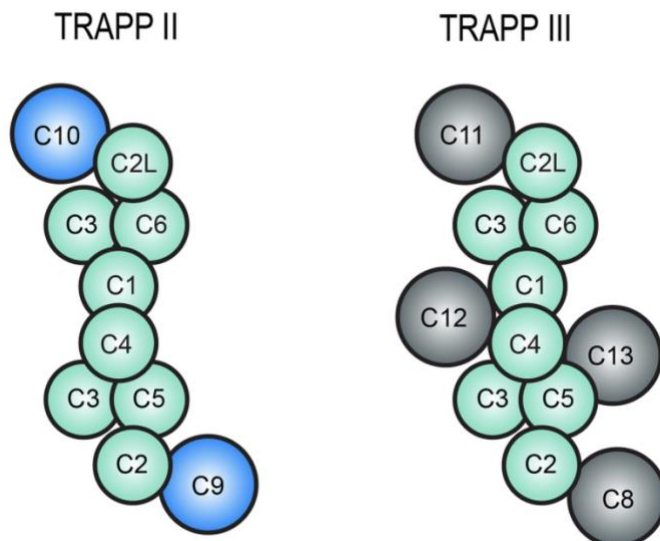


Figure 1.1. **A schematic representation of TRAPP II and TRAPP III mammalian complexes.** The common core of 7 distinct proteins is indicated in green. TRAPP II has two additional subunits, indicated in blue. TRAPP III has four additional subunits, indicated in gray. Reproduced from Sacher et al., 2019.

Both the yeast and human TRAPP III complex has been implicated in various cellular processes including ER-to-Golgi trafficking (Joiner et al., 2021; Scrivens et al., 2011; Zhao et al., 2017) and autophagy (Behrends et al., 2010; Brunet et al., 2013). A cryogenic electron microscopy

(cryo-EM) structure of the TRAPP III complex has been elucidated for the *Drosophila* complex, which suggests how the core and subunit-specific proteins arrange to form TRAPP III (Galindo et al., 2021). In the TRAPP III complex, the structure suggests that TRAPPC8 and TRAPPC11 hold the complex together like a clasp, which is an interesting finding considering that these two subunits are known to be essential for cell viability (Blomen et al., 2015; Hart et al., 2015; Wang et al., 2015). The essentiality of the TRAPPC11 protein in mammals presses for a more thorough investigation of the function of the protein and characterization of genetic mutations.

1.3 TRAPPC11 Mutations in Human Diseases

TRAPPC11 is an essential protein that is increasingly being discovered to be associated with human diseases. The protein is 1133 amino acids long and has two highly conserved regions (Bögershausen et al., 2013; Scrivens et al., 2011). The first region of 258 amino acids is referred to as the foie gras domain (Bögershausen et al., 2013; Scrivens et al., 2011) and the second is a carboxy-terminal region of 59 amino acids referred to as the gryzun domain (Milev et al., 2019). The foie gras domain appears to be of critical importance as a mutation within this region leads to a loss of detectable amounts of the protein (Bögershausen et al., 2013). Notably, many mutations fall around the gryzun region, suggesting the carboxy terminus is also of importance (Figure 1.2) (Milev et al., 2019).

The TRAPPC11 protein has been implicated to function in Golgi apparatus morphology (Scrivens et al., 2011), ER-to-Golgi membrane trafficking (Scrivens et al., 2011; Zhao et al., 2017) COP II recruitment to the ER (Zhao et al., 2017), N-linked protein glycosylation (DeRossi et al., 2016), and autophagy (Stanga et al., 2019).

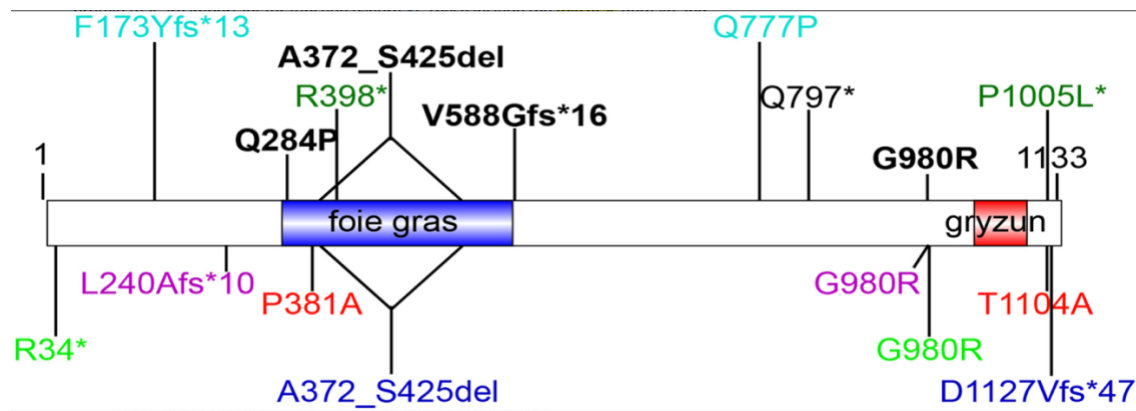


Figure 1.2. **A schematic of the TRAPPC11 protein and known mutations.**

There are two highly conserved regions: the foie gras region of 258 amino acids, represented in blue, and the gryzun region of 59 amino acids, represented in red. Indicated are the different mutations that have been reported to date. Mutation A372_S425del is present in both *TRAPPC11* patients reported in this paper, B18 and B19. Reproduced from Sacher et al., 2019.

Mutations within TRAPPC11 not only exhibit defects in these cellular processes, but also exhibit clinical phenotypic variations such as muscular dystrophy, as well as liver, ocular and brain pathologies (Bögershausen et al., 2013; Fee et al., 2017; Koehler et al., 2017; Larson et al., 2018; Liang et al., 2015; Matalonga et al., 2017; Milev et al., 2019; Munot et al., 2022)

The work herein will focus on two individuals with biallelic TRAPPC11 mutations. The first, referred to as B18, has a compound heterozygous mutation c.[1287+5G>A];[2407C>T] p.[(Ala372_Ser429del)];[(Gln803*)]. While the former variant was previously described (Bögershausen et al., 2013), the latter is novel. The second will be referred to as B19 and has a compound heterozygous mutation c.[371_374delTCAG];[1287+5G>A] p.[(Val124Glyfs*15)];[Ala372_Ser429del]. Both contain the 1287+5G>A mutation, which results in a splice variant, leading to an in-frame deletion of 58 amino acids within the foie gras domain (Bögershausen et al., 2013). The primary difference between the B18 and B19 variants is

that B18 has an allele with a nonsense mutation and B19 has a frameshift. This provides the opportunity to study the potential read-through of a nonsense mutation by having cells that should show some degree of improvement (B18) compared to the allele with the frameshift (B19).

1.4 Autophagy

As stated above, TRAPPC11 is implicated in autophagy, a cellular process that utilizes the efficiency of membrane trafficking to maintain cellular homeostasis (Boya et al., 2013). It is a pathway that ultimately eliminates unwanted or harmful cytoplasmic components and is upregulated during cell differentiation, times of protection against disease or infection, and times of stress, such as starvation (Søreng et al., 2018). The autophagic pathway begins with the nucleation of the isolation membrane into a double membrane structure (Rubinsztein et al., 2012). The closing of the isolation membrane results in an autophagosome, a structure that fuses with a lysosome to form an autolysosome that enables degradation of cytoplasmic components (Eskelinen, 2005).

Important proteins that help regulate the process of autophagy in eukaryotes are LC3-I and LC3-II. LC3 is modified endogenously by a ubiquitylation-like system (Tanida et al., 2005). During the onset of the autophagic pathway, the carboxy-terminus of LC3 is cleaved, creating a more soluble form of the protein, referred to as LC3-I (Kabeya, 2000; Sagiv, 2000; Tanida et al., 2003). The LC3-I form of the protein is then lipidated to form LC3-II, which binds to autophagosomes and autolysosomes. Hence, LC3-II is an accepted indicator of autophagy (Kabeya, 2000).

Another protein that is important in the autophagic pathway is ATG2. This protein is required for isolation membrane expansion and it interacts with a phosphatidylinositol-3-phosphate (PI3P) effector, WIPI4 (Velikkakath et al., 2012; Zheng et al., 2017). The mechanism of closure of an isolation membrane into an autophagosome is not fully understood. However, LC3 and ATG proteins are implicated in this process (Kishi-Itakura et al., 2014).

As mentioned previously, the TRAPP III complex, including TRAPPC11, has been implicated in the process of autophagy. The different complex-specific proteins within the TRAPP III complex function in different steps of the autophagic pathway. Specifically, TRAPPC8 affects the formation of the isolation membrane, TRAPPC11 is required for the closure of the isolation membrane, and TRAPPC12 is required after TRAPPC11, but its exact function is not yet fully understood (Stanga et al., 2019). In TRAPPC11 deficient cells, there is an increase in LC3-positive membranes that cannot be cleared due to the inability to close the isolation membrane. In addition, TRAPPC11 was found to interact with ATG2B (an ATG homolog) and WIPI4, thus reinforcing its function in isolation membrane growth and closure (Stanga et al., 2019). Known TRAPPC11 deficient individuals are ideal candidates for further investigation of the role of TRAPP III in autophagy.

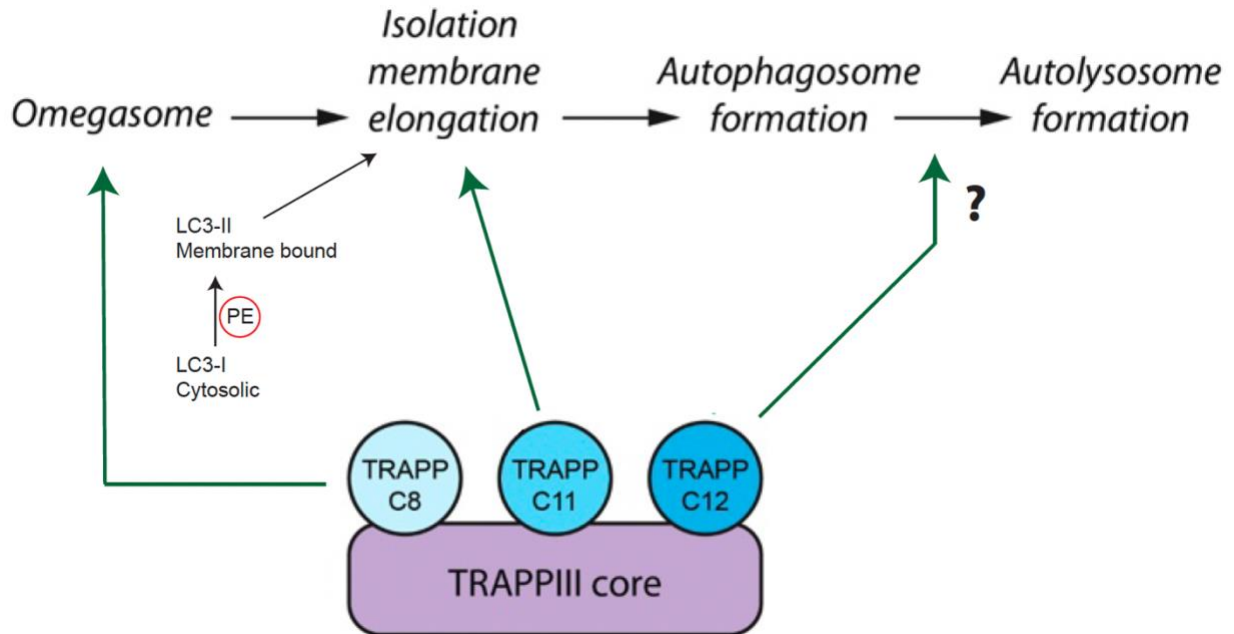


Figure 1.3. A representation of the TRAPP III proteins in autophagy.

The TRAPP III complex is known to function in autophagy and three of the complex-specific proteins depicted have implicated functions in different stages of the pathway. TRAPP C11 was shown to function upstream of autophagosome formation while TRAPP C8 functions much earlier in the pathway. The function of TRAPP C12 is not fully understood, but is shown to function after autophagosome formation. LC3-I protein is a cytosolic protein which, when lipidated with phosphatidylethanolamine (PE), forms LC3-II and associates with the isolation membrane. LC3-II can be identified once isolation membrane elongation begins. This figure was adapted from Stanga et al., 2019.

1.5 Nonsense mutations

As mentioned above, the B18 primary cells contain a nonsense mutation as one of the TRAPP C11 alleles. A nonsense mutation is a nucleotide change that can alter a codon, resulting in a nonsense codon, or a premature stop codon. This type of mutation often leads to premature termination of protein translation, which can result in a shorter, less-functional or completely non-functional protein product (Michorowska, 2021). Normal protein translation begins by a ribosome reading mRNA from the 5' end to the 3' end (Nagel-Wolfrum et al., 2016). In essence, a ribosome begins by reading mRNA from the 5' end to the 3' end. During this process, transfer

RNA (tRNA) rests at the P site of the ribosome and the next codon to be read rests at the A site of the ribosome (Figure 1.3). Normal protein translation ends when the naturally occurring stop codon is reached at the 3' end of the coding sequence. The end of protein translation requires two termination factors: eukaryotic release factors 1 and 3 (eRF1 and eRF3) (Nagel-Wolfrom et al., 2016). eRF1 functions to recognize the stop codon and eRF3 is a GTPase that functions to assist the termination process (Peltz et al., 2013). A nonsense codon that arises during the process of protein translation often results in premature termination of protein translation.

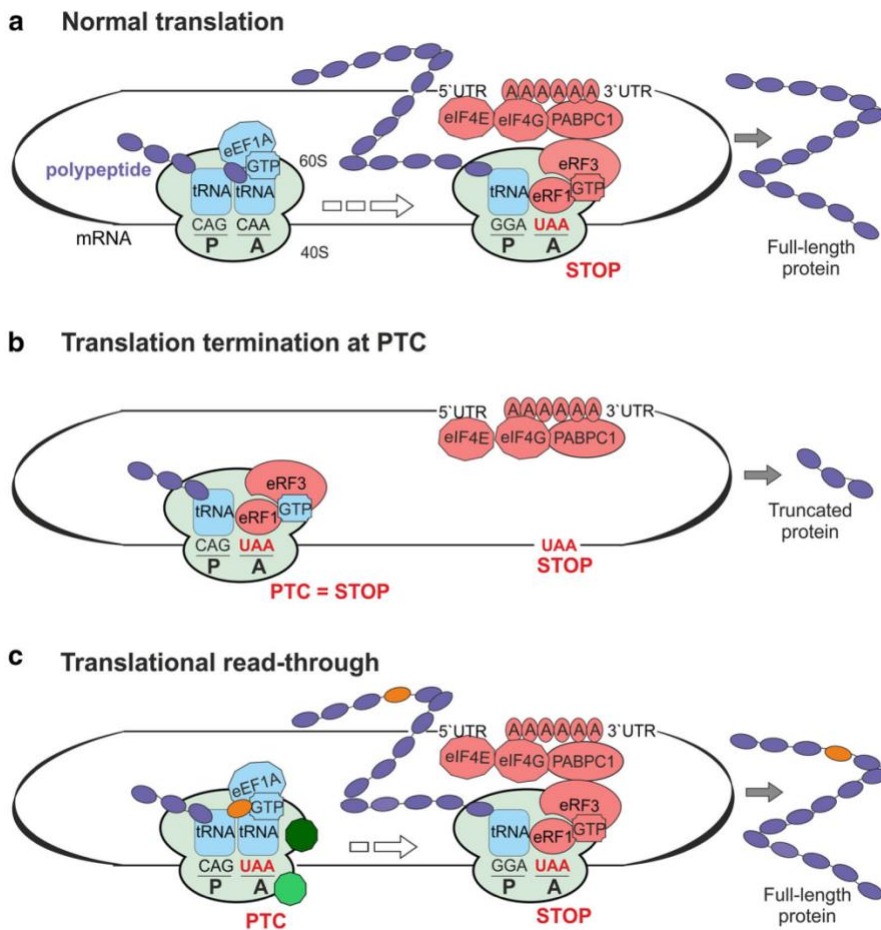


Figure 1.4. **A representation of normal protein translation in comparison to translation that is hindered due to a nonsense mutation.** The ribosome is indicated in a light green color. There are two sites of the ribosome: A and P. The P site of the ribosome is where the growing polypeptide chain lies. The A site of the ribosome is where the next codon to be read resides. Translational read-through inducing drugs (TRIDs) will bind to the A site of the ribosome to either introduce a near-cognate tRNA, or hinder the eRF1 and eRF3 complex from terminating translation. The light green octagon is representative of where an aminoglycoside antibiotic

would bind to the ribosome. The dark green octagon is representative of where Ataluren would bind to the ribosome. It is currently unclear how Amlexanox interacts with the ribosome. Reproduced from Nagel-Wolfrum et al., 2016.

Oftentimes, a nonsense mutation leads to a process referred to as nonsense mediated mRNA decay (NMD). This is a cellular control mechanism that rapidly degrades mRNA transcripts that harbor a nonsense codon (Maquat, 2004). NMD is capable of recognizing the stalled or colliding ribosomes near the premature stop codon to ensure the decay of only nonsense codon-bearing mRNA (Lejeune, 2017). To date, there are about 7,000 human genetic diseases that have been characterized, and nearly 12% of the diseases can be attributed to nonsense mutations (Ng et al., 2021).

1.6 Translational Read-through Inducing Drugs (TRIDs)

Given the abundance of human disease caused by nonsense mutations, the ability to read through such mutations to the normal stop codon could prove beneficial from a therapeutic standpoint. There are a variety of translational read-through inducing drugs (TRIDs) that are being investigated to understand their read-through capabilities and effectiveness. Aminoglycoside antibiotics have been used the longest and therefore have the most research supporting their read-through abilities. Aminoglycoside antibiotics are polar compounds that are known to be highly effective in their read-through capabilities. However, they can pose severe toxic effects such as retinal toxicity and nephrotoxicity most likely due to their read-through of normal stop codons (Vössing et al., 2020). Aminoglycoside antibiotics have been shown to function in read-through by binding to the A site of the ribosome, introducing a near-cognate tRNA, and promoting elongation of the growing polypeptide (Ng et al., 2021). In order to find a safe way to

therapeutically read through nonsense mutations, there was a need for new, less toxic, compounds. Two such TRIDs are Ataluren and Amlexanox. Both drugs have read-through properties comparable to aminoglycoside antibiotics but have proven to be less toxic.

Ataluren falls under the class of oxadiazoles and is a hydrophobic small molecule that has been shown to stimulate nonsense codon read-through (Ng et al., 2021). Ataluren (also known as Translarna or PTC124) has been approved for use by the European Medicines Agency and is currently being used to treat individuals with nonsense mutation-mediated Duchenne muscular dystrophy (Michorowska, 2021). Ataluren has been suggested to function by completely inhibiting the eRF1/eRF3-dependent peptidyl-tRNA hydrolysis, thus preventing the release of the ribosome and growing peptide and stimulating the read-through of a nonsense codon (Ng et al., 2021).

Amlexanox falls under the NMD inhibitor class of read-through inducing drugs. Presently, Amlexanox is not being used to treat nonsense mutation-mediated diseases, but this drug was used in the past to treat other pathologies such as mouth ulcers and asthma (Atanasova et al., 2017; Eintracht et al., 2021; Gonzalez-Hilarion et al., 2012). Using NMD inhibitors to treat nonsense mutation-mediated diseases was sought after due to the limited efficiency of therapeutic read-through seen by aminoglycosides and Ataluren (Bidou et al., 2004; Welch et al., 2007). The ability of Amlexanox to inhibit NMD was discovered using a luciferase-based screen, where it showed an ability to stabilize nonsense mutation-bearing mRNA in addition to its ability to stimulate read-through of the nonsense codon (Eintracht et al., 2021; Gonzalez-Hilarion et al., 2012). The mechanism of action is not yet understood.

1.7 Objective

The TRAPP family of complexes is beginning to gain recognition for its role in a variety of neurodevelopmental disorders. Not only is it crucial to study genes that are implicated in life-altering diseases, but finding a way to treat them is equally as important. Nonsense mutation-mediated diseases are ideal candidates for drug developmental research due to their ability to be treated with TRIDs.

Two lines of patient-derived fibroblasts will be studied here; B18 and B19. Both individuals have compound heterozygous mutations in the TRAPPC11 gene and therefore are impacted by the detriment of neurodevelopmental disorders. I will assess the ability of Ataluren and Amlexanox to rescue any cellular defects detected. To this end, I will first characterize the cellular defects for each line of fibroblasts. I will then assess the ability of these defects to be rescued by either Ataluren or Amlexanox treatment.

2. MATERIALS AND METHODS

2.1 Cell Culture

HeLa cells and primary fibroblasts were cultured in Dulbecco's modified eagle medium (DMEM) (Wisent, St. Bruno, Quebec, Canada) supplemented with 10% (vol/vol) fetal bovine serum (FBS; Thermo Fisher Scientific, Waltham, Massachusetts) at 37°C in a humidified incubator with 5% CO₂. Cells were treated with TRIDs when they reached 80% confluency. Cells were harvested 48h after TRID treatment.

2.2 Starvation Treatments

Primary fibroblasts were seeded in 6-cm diameter dishes, washed twice with phosphate buffered saline (PBS) and incubated with Earl's balanced salt solution (EBSS) (Wisent, St. Bruno, Quebec, Canada) for 0h, 1h and 2h. The cells were lysed by harvesting in lysis buffer (150 mM NaCl, 50 mM Tris pH 7.2, 1 mM DTT, 1% Triton X-100, 0.5 mM EDTA, Complete protease inhibitors (Roche, Basel, Switzerland)) and analyzed by western blotting.

2.3 Translational Read-Through Drugs (TRIDs)

Ataluren (PTC124) from Selleckchem was dissolved in dimethyl sulfoxide (DMSO). Cells were treated with Ataluren at a concentration of 5 µg/mL for 48h. Amlexanox was purchased from Toronto Research Chemicals Inc. and dissolved in DMSO. Cells that were treated with Amlexanox were treated with a concentration of 250 µM for 48h.

2.4 Antibodies and Dyes

The antibodies used were rabbit anti-LC3 (1:2500) (Abcam, Cambridge, MA), mouse anti-tubulin (1:10000) (Sigma-Aldrich, St. Louis, MO), rabbit anti-mannosidase II (1:500) (gift from Dr. Kelly Moreman, University of Georgia), and mouse anti-HA.11 (1:1000) (Covance, Princeton, NJ). DNA was visualized by staining with Hoechst 33342 (1:2000) (Invitrogen, Waltham, MA). Anti-LC3, anti-tubulin, and anti-HA.11 were used for western blotting. Anti-mannosidase II and Hoechst were used for immunofluorescence microscopy.

2.5 Immunofluorescence microscopy

The fibroblasts were gently washed twice with PBS, fixed with 4% paraformaldehyde (PFA) for 15 minutes at room temperature, quenched with 0.1M glycine for 10 minutes and permeabilized with 0.1% Triton X-100 for 7 minutes. The cells were blocked in 5% normal goat serum in PBS for 45 minutes at room temperature. Primary antibodies were diluted in 5% normal goat serum and were added to coverslips and incubated overnight at 4°C. Cells were then washed twice for 10 minutes each time with PBS. Secondary antibodies were diluted in 5% normal goat serum in PBS and applied for 45 minutes at room temperature. The coverslips were washed once with Hoescht (1:2000) in PBS for 2 minutes, then twice for 10 minutes each with PBS. The coverslips were then mounted with Prolong Gold AntiFade (Life Technologies, Carlsbad, CA). Images were recorded on a Nikon confocal laser scanning microscope C2 TIRF fitted with a 40X objective lens (numerical aperture (NA) 1.49). The Golgi fragmentation images were acquired with 0.20 μm increment size. ImageJ was used to delineate 257 cells. The N values for control, control + Ataluren, and control + Amlexanox are 33, 30 and 30, respectively. The N values for B18, B18 + Ataluren, and B18 + Amlexanox are 29, 32, and 24, respectively. The N values for

B19, B19 + Ataluren, and B19 + Amlexanox are 23, 25, and 31, respectively. Images were then converted to IMS files and imported to Imaris. Imaris was set to identify Golgi structures as spherical structures no smaller than 0.550 μm in size. The number of fragments that fit this description within the cell were then identified and listed, along with their area, but only the number of fragments per cell was used for this experiment.

2.6 Western blotting

Samples (20 μg total protein for all proteins) were fractionated on 8 or 15% SDS-polyacrylamide gels for 1 hour and 30 minutes at 110V. The proteins were transferred to nitrocellulose membranes (BioRad, Hercules, California) for 1 hour at 100 V in transfer buffer (composition: 25mM Tris, 192mM Glycine, and 20% methanol [vol/vol]). Membranes were blocked with 5% skim milk powder in PBS-T (PBS with 0.1% Tween 20 [vol/vol]) for 1 hour. Primary antibodies were incubated in PBS-T overnight at 4°C and secondary antibodies were incubated for 1 hour at room temperature. Primary antibody dilutions were as follows: anti-LC3 was diluted 1:2500; anti-HA.11 was diluted (1:2000). Membranes were then incubated with ECL reagent (Thermo Fisher, Waltham, MA) for one minute and detected using an Amersham Imager 600.

2.7 Retention using selective hooks (RUSH) assay

Fibroblasts were maintained in DMEM supplemented with 10% fetal bovine serum (FBS). In order to examine ER-to-Golgi trafficking, the RUSH assay was performed as previously described (Boncompain et al., 2012) and quantified with ImageJ. Briefly, this assay involves a reversible interaction with a stably anchored hook protein that is fused to streptavidin and a reporter protein that is fused to a streptavidin-binding peptide. The addition of biotin initiates the

release of the reporter protein from the hook protein at the donor compartment and subsequent transport to the acceptor compartment. Here, fibroblasts were transfected via electroporation with a fluorescent cargo protein (Sialyl transferase (ST)-eGFP) that is retained in the ER until the cells are exposed to biotin. The fluorescent cargo protein was observed as it exits the ER and arrives at the Golgi. Individual cells were quantified with ImageJ. In ImageJ, the Golgi was identified in the cell to be quantified. The Golgi was manually outlined, and the fluorescence intensity was measured for each time point in the movie (images were captured every two minutes). An arbitrary spot was chosen as “background” using the same Golgi outlining. The fluorescence intensity from the Golgi at each time point was subtracted from the “background” value. Next, the entire cell was outlined, and the fluorescence intensity was measured for each time point. A “background” measurement was taken here, as well, with the same cell outlining. The background-corrected Golgi fluorescence intensity was then divided by the background-corrected total cell fluorescence intensity that corresponds to each time point. The remaining values (the ratio of Golgi fluorescence intensity / total cell fluorescence intensity) are the values that are plotted on the graph.

2.8 DNA constructs

A human TRAPPC11 cDNA was used for the generation of an N-terminal HA tagged, C-terminal Myc tagged reporter construct (forward

primer: 5'-ACT TAA GCT TGG TAC CGA GCT CGG ATC CAC CAT GTA CCC ATA CGA TGT TCC AGA TTA CGC TAT GAG CCC CAC ACA GTG GGA CTT-3', reverse primer: 5'-CGC CAC TGT GCT GGA TAT CTG CAG AAT TCT CAC AGA TCC TCT TCT GAG ATG AGT TTT TGT TCT TCA CTA GCA CTC TCT CCA GTC TG-3'). The wild-type construct

was inserted into the BamHI/NotI restriction sites of the pcDNA3.1+ vector (Invitrogen, Waltham, MA). The nonsense mutation 2407C>T for *TRAPPC11* was generated by site-directed mutagenesis using Pfu TURBO DNA polymerase (Agilent, Santa Clara, CA). Primers for site-directed mutagenesis were: forward 5'-GGA TGC CAA TTT AAC TTA GAA GAC TCA CGT GAC-3' and reverse 5'-GTC ACG TGA GTC TTC TAA GTT AAA TTG GCA TCC-3'.

3. RESULTS

3.1 Clinical summary of TRAPPC11 individuals B18 and B19

There are two individuals harboring *TRAPPC11* mutations studied within this thesis. A brief background of their clinical phenotypes is presented below.

B18: This individual was 25 months of age at the time of the exam. The initial concern for him was his failure to thrive at 5 months. Subsequently, low muscle tone and motor delay was observed. At 8 months, the individual had febrile status epilepticus with subsequent regression and visual impairment. Dysphagia required a G tube placement for feeding. This individual also exhibited axial hypotonia and appendicular hypertonia. The best motor development observed was at 8 months, he almost sat without a support, held a bottle, rolled over, fixed and followed, and babbled.

B19: Pregnancy for this individual was uncomplicated, with the only issue being neonatal jaundice which was treated with phototherapy. Prior to 6 months of age, she met her milestones. The first concerns at 6 months presented as an unprovoked seizure, stiffening and cyanosis. An EEG showed epileptiform activity. A CT and subsequent brain MRIs were completed at 8 months then 3 years which revealed significant progressive atrophy due to loss of grey and white matter, the latter being more prominent which is consistent with leukodystrophy. She developed progressive spasticity and worsening axial hypotonia after 6 months of age and her stridor was treated with laryngoplasty at 8 months. The individual suffered from dysphagia and her failure to thrive required a G tube placement at 4 years of age. Over time, she stopped fixing and following with nystagmus and roving eye movements. The individual suffered from sleep apnea and used a

nocturnal CPAP. Progressive thoracic scoliosis was present at the time of her exam and leg length discrepancy was observed, likely from hip dysplasia/dislocation. This individual was non-verbal, did not reach, fix or follow. She did make eye contact and tracked prior to the onset of seizures at 6 months. The best motor development observed was her ability to sit with support, hold her head up for a few seconds, and could take a few steps when significantly supported.

This individual had a brother with the same *TRAPPC11* mutations that passed away in his sleep at 3 years of age. The brother exhibited abnormal development that was noticed at his 6 months visit. There was a history of abnormal EEG but no clinical seizures. His brain MRI showed white and grey matter atrophy. Progressive spasticity and dysphagia required G-tube placement. A summary of the clinical features is presented in Table 3.1. Whole exome trio sequencing revealed biallelic compound heterozygous mutations in both *TRAPPC11* patients with each parent carrying one allele: B18 c.[1287+5G>A];[2407C>T] p.[(Ala372_Ser429del)];[(Gln803*)] and B19 c.[371_374delTCAG];[1287+5G>A] p.[(Val124Glyfs*15)];[Ala372_Ser429del].

The fibroblasts from these two individuals will be used throughout the rest of this thesis.

Patient ID	Patient B18	Patient B19	Brother of B19
Sex	M	F	M
Age at follow-up (death)	25 month	6 yrs	died age 3 yrs
<i>TRAPPC11</i> mutation	c.[1287+5G>A];[2407C>T]	c.[371_374delTCAG];[1287+5G>A]	c.[371_374delTCAG];[1287+5G>A]
	p.[(Ala372_Ser429del)];[(Gln803*)]	p.[(Val124Glyfs*15)];[Ala372_Ser429del]	p.[(Val124Glyfs*15)];[Ala372_Ser429del]
First symptoms (age, which)	5mo, failure to thrive, gross and fine motor delays	4mo, hypotonia and seizures	6mo, failure to thrive, elevated liver function tests and developmental delays
Psychomotor/developmental delay	+	+	+
Intellectual disability - IQ (age)		non verbal	non verbal
Ataxia (age at diagnosis)	n/a	n/a	n/a
Hypotonia		+	+ (never ambulatory)
Seizures/EEG (age at onset)	+ (7mo)	+ (4mo, epileptiform discharges)	+ (20mo, bilateral temporal epileptiform discharges L>>R)
Cerebral atrophy	+ (1yr/6 mo)	+ (7mo)	
Cerebellar atrophy	+ (1yr/6 mo)	- (7mo)	
White matter loss	+ (occipital and right posterior temporal, 1yr/6 mo)	+ (leukodystrophy, 7mo)	+
Gray matter loss	-	+ (7mo)	
Corpus callosum anomalies	+ (thinning of body and splenium, 7m/25d)	- (7mo)	
Diagnosis (i.e. CMD, LGMD, etc)	CMD		mitochondrial disorder NOS
Elevated CK	+ (306-2899 UI/L)	+ (2500 UI/L)	+ (1024 UI/L)
Cortical visual impairment	+ (poor tracking, optic pallor)	+ (Inconsistent tracking and focussing)	+
Scoliosis	+ (mild right convex thoracolumbar)	+ (thoracic)	-
Gastrointestinal impairment			+ (GERD and g-tube placement)
Other		Congenital torticollis	Improvement of gross motor skills: better neck control and standing longer without support; not ambulatory

Table 3.1. **Summary of clinical phenotypes in three TRAPPC11 patients**

Abbreviations: EEG, Electroencephalogram; CMD, congenital muscular dystrophy; LGMD, limb-girdle muscular dystrophy; CK, creatine kinase; NOS, not otherwise specified; GERD, gastroesophageal reflux disease

3.2 Cryo-EM structure of TRAPPC11 and location of mutations

The structure of TRAPPC11 was elucidated via cryo-EM by Galindo et al., 2021. The N-terminus of the TRAPPC11 protein was described, but the C-terminus was unable to be fully resolved. As shown in Figure 3.1, the foie gras domain resides at the amino terminal end of the TRAPPC11 protein.

Both individuals described here (B18 and B19) have the c.[1287+5G>A] mutation, which results in a splice variant, leading to an in-frame deletion of 58 amino acids within the foie gras domain. This area is indicated by the red arrow in Figure 3.1. B19 has a second mutation c.[371_374delTCAG] which is a frameshift also found within the amino terminal region of the protein. The amino terminus of TRAPPC11 is shown to interact with TRAPPC2L and TRAPPC3. B18 has a nonsense mutation c.[2407C>T] that is found near the carboxy terminal region of the protein, indicated by a black arrow in Figure 3.1. The carboxy terminal region interacts with TRAPPC12 and TRAPPC13. Both B18 and B19 have mutations near the amino terminus, but only B18 has a mutation near the carboxy terminus.

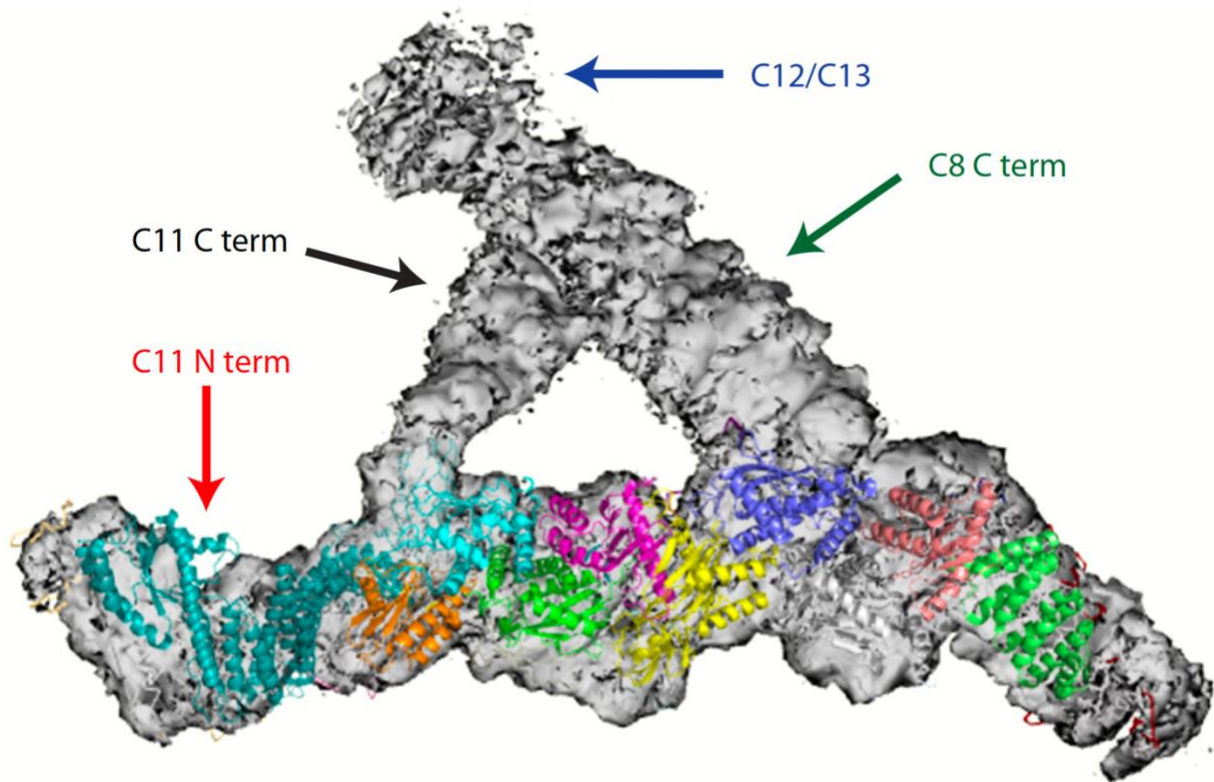


Figure 3.1 **Cryo-EM structure of TRAPP III.** Shown is an electron density map for the TRAPP III complex with the electron densities in gray. Superimposed is resolved 3D structures of the proteins listed below. The N-terminus of TRAPPC11 is indicated by the red arrow (C11 N term). The C-terminus of C11 is indicated by the black arrow (C11 C term). The undefined region of TRAPPC12 and TRAPPC13 is indicated by the blue arrow (C12/C13). The C-terminus of TRAPPC8 is indicated by the green arrow (TRAPPC8 C term). The proteins (other than TRAPPC12 and TRAPPC13) are indicated by a color. From left to right: TRAPPC11 is indicated in cyan, TRAPPC2L is orange, TRAPPC6 is light blue, TRAPPC3 is green, TRAPPC4 is yellow, TRAPPC1 is pink, TRAPPC4 is yellow, TRAPPC3 is purple, TRAPPC5 is gray, TRAPPC2 is light pink and lastly TRAPPC8 is green. The C-terminus of TRAPPC8 extends to TRAPPC12 and TRAPPC13 and the N-terminus is in green.

3.3 Autophagy protein LC3-II is elevated in TRAPPC11 individual B18, but not in B19

It was previously reported that TRAPPC11 functions in autophagy, specifically in the sealing of the autophagosome isolation membrane (Stanga et al., 2019). Both TRAPPC11 cells B18 and B19 had not yet undergone any experimental studies to characterize their cellular defects, including autophagy. I first characterized the cells for an autophagic defect by using a well-

established starvation assay. The assay deprives the fibroblasts of nutrients and serum, which allows for the observation of endogenous LC3-II via western blotting. Without the use of nutrient deprivation, LC3-I and -II protein levels are unpredictable and hard to interpret (Klionsky et al., 2021).

To begin, control, B18 and B19 fibroblasts were starved for up to two hours in EBSS starvation medium to trigger autophagy. The cell lysates were then collected at three different time points - 0h, 1h and 2h. As seen in Figure 3.2A and quantified in Figure 3.2B, in the control cells there is an increase of LC3-II protein over the 2 hour period. In contrast, B18 exhibited a statistically significant increase in the level of LC3-II protein at each time point compared to the control. In the B18 cells, the LC3-II protein began at a much higher level and remained relatively steady at this higher level throughout the starvation period. In addition, the level of LC3-II protein in B18 fibroblasts was significantly higher than the level in B19 fibroblasts. The B19 fibroblasts did not show significant differences in the level of LC3-II protein over 2 hours compared to the control. It is worth noting that there could be alternative defects in autophagy in the B19 cells, but for this experiment, the cells do not exhibit a significant difference in autophagic flux compared to the control.

and probed for LC3B and tubulin. A) Representative western blots for each condition. The LC3-I and LC3-II band labelling is located to the right. LC3-I is found at ~17 kDa and LC3-II is found at ~15 kDa. B) Quantification of the western blots with the LC3-II signal normalized to the tubulin loading control (shown under each LC3 blot in A). Quantification was done with ImageJ. There is strong statistical significance ($p \leq 0.0001$) between B18 and B18 +ata, +aml. There is no statistical significance between B19 and B19 +ata, and weak significance ($p \leq 0.05$) between B19 and B19 +aml. Statistical significance was assessed using two-way ANOVA with posthoc Tukey HSD analysis. The error bars indicate SEM. Ata represents Ataluren and Aml represents Amlexanox.

3.4 TRID treatment rescues the autophagic defect in TRAPPC11 B18 cells, but not in B19 cells

The clear autophagic abnormalities seen in the B18 cells as well as the nonsense mutation allele provide an optimal setting to study the effectiveness of TRID treatments. Ataluren has been used in various studies, with positive results. The drug is also being studied in a phase 3 clinical trial in the USA for the treatment of Duchenne Muscular Dystrophy (<https://clinicaltrials.gov/ct2/show/study/NCT01826487>). In addition, Amlexanox has recently been used in terms of read-through treatment.

The fibroblasts were subject to a starvation assay as stated above. In this case, the cells were treated with Ataluren (5 $\mu\text{g}/\text{mL}$) or Amlexanox (250 μM) for 48h prior to the starvation assay and lysate collection. As expected, the control cells had no alterations in the level of LC3-II protein after 48h of TRID treatment (Figure 3.2A,B). B19 fibroblasts also showed no statistically significant alterations after treatment with Ataluren, but showed a slight increase in the level of LC3-II protein after being treated with Amlexanox. The increase is less significant than the changes seen in B18, and there is no significant difference between B19 and the control. Interestingly, B18 fibroblasts showed a noticeable decrease in the LC3-II protein at all time

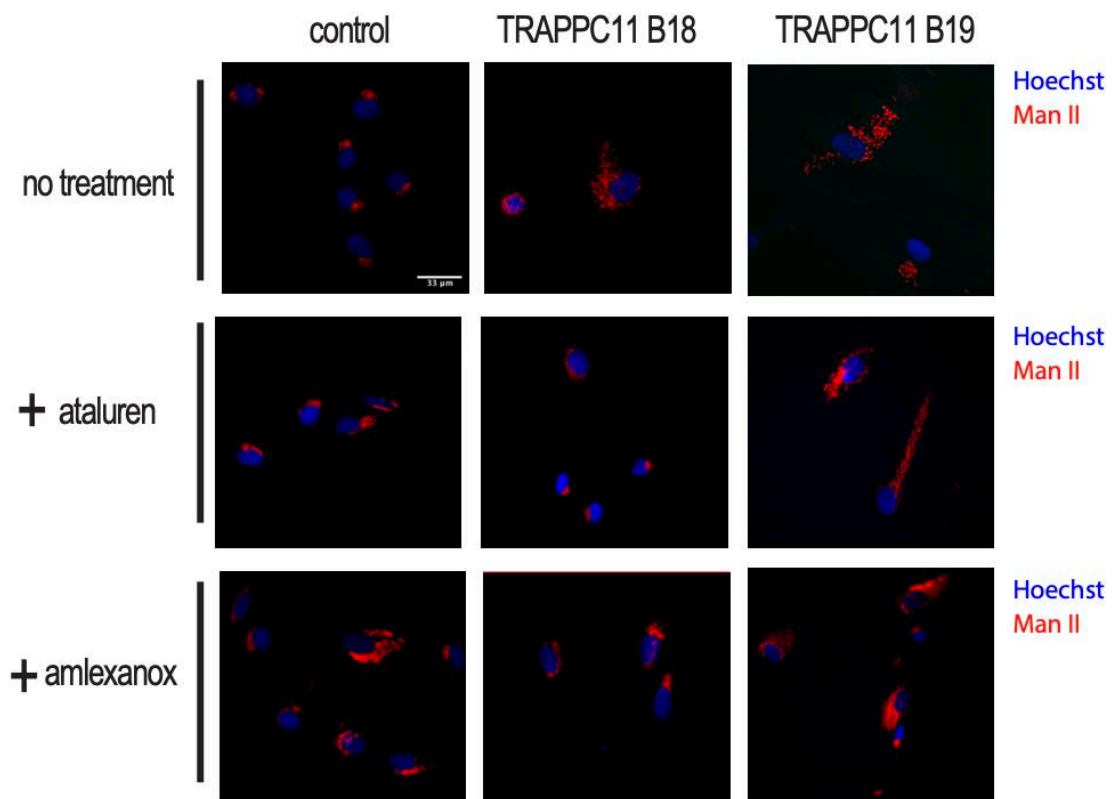
points after treatment with Ataluren and Amlexanox (Figure 3.2A). The quantification of these results indicated a statistically significant decrease in LC3-II levels in B18 after treatment with either Ataluren or Amlexanox, with a pattern more similar to control cells (Figure 3.2B). There was no significant change in the level of LC3-II protein in B19. The results suggest that Ataluren and Amlexanox recovered some wild-type functionality of autophagy based on the LC3-II protein assay. Based on the results of the starvation assays, I conclude that Ataluren and Amlexanox both rescued wild-type function of the *TRAPPC11* nonsense mutation c.2407C>T allele in the B18 patient fibroblasts.

3.5 Number of Golgi fragments per cell in B18 cells decreased with TRID treatment

Not only is TRAPPC11 known to have a role in autophagy, but its absence is associated with changes in Golgi morphology. Individuals with a mutation in TRAPPC11 or in cells where the protein has been knocked down by RNA interference display highly fragmented Golgi to varying degrees (Bögershausen et al., 2013; DeRossi et al., 2016; Milev et al., 2019; Scrivens et al., 2011). With this in mind, the degree of Golgi fragmentation in B18 and B19 cells was compared to that of the control. The Golgi was visualized using antibodies that recognize mannosidase-II (man-II) and p115, both Golgi-resident proteins.

Both B18 and B19 exhibited significantly more fragmented Golgi compared to the control (Figure 3.3A). On average, a control cell had 13 ± 1.5 Golgi fragments, a B18 cell had 52 ± 5.4 fragments, and a B19 cell had 33 ± 6.1 fragments. Compared to the control cells, there was a statistically significant increase in the number of Golgi fragments per cell in both B18 and B19 fibroblasts compared to control (Figure 3.3B).

A



B

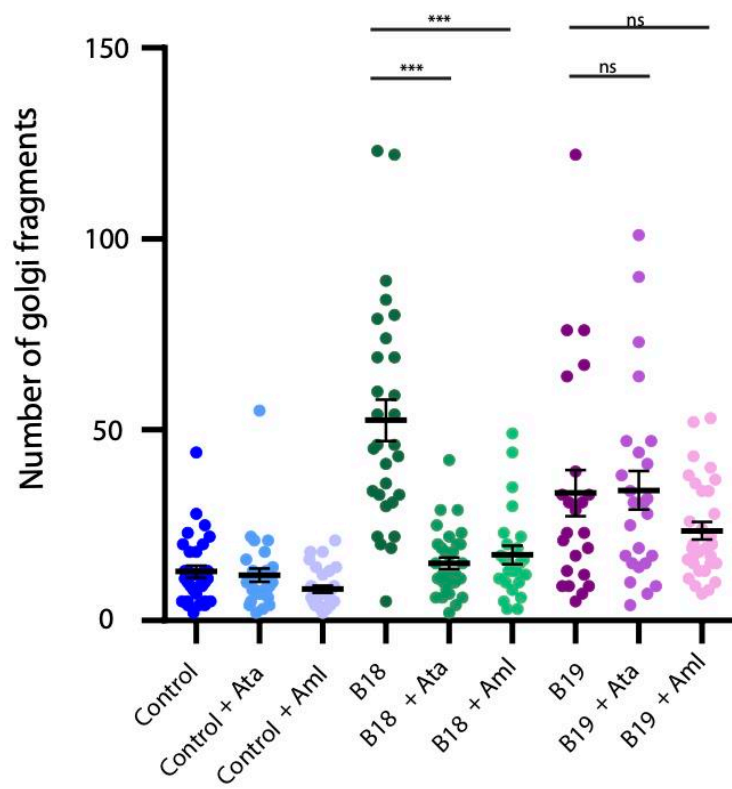


Figure 3.3. Golgi fragmentation decreases in cells from patient B18 following TRID treatment. A) Fibroblasts from control, B18 and B19 were either untreated, treated with Ataluren for 48h or treated with Amlexanox for 48h. Then the fibroblasts were fixed and stained for Man-II and Hoechst. B) Golgi fragments per cell were quantified using Imaris. Statistical significance was assessed using one-way ANOVA with posthoc Tukey HSD analysis. The error bars indicate SEM. The N values for control, control + ata, and control + aml are 33, 30, and 30, respectively. The N values for B18, B18 + ata and B18 + aml are 29, 32, and 24, respectively. The N values for B19, B19 + ata, and B19 + aml are 23, 25 and 31, respectively.

I then examined the effects of Ataluren and Amlexanox treatment on the Golgi fragmentation.

As above, the fibroblasts were treated with Ataluren and Amlexanox for 48h prior to fixation and staining. While the control and B19 cells did not show any significant changes in Golgi fragmentation per cell after treatment, B18 cells showed a significant decrease in the number of Golgi fragments per cell after treatment with either Ataluren or Amlexanox. The average number of Golgi fragments per cell in the control after treatment with Ataluren and Amlexanox were 12 ± 1.8 and 8 ± 0.9 , respectively. The average number of Golgi fragments per cell in B19 after treatment with Ataluren and Amlexanox were 34 ± 5.1 and 24 ± 2.3 , respectively. Lastly, the average number of Golgi fragments per cell in B18 after treatment with Ataluren and Amlexanox were 15 ± 1.5 and 17 ± 2.4 , respectively. The B18 cells improved from an average of 52 Golgi fragments per cell to about 15-17 after treatment. The results obtained from the Golgi fragmentation analysis suggests Ataluren and Amlexanox both rescue the Golgi morphological defect in B18 cells.

3.6 Ataluren rescues membrane trafficking defect in B18 fibroblasts

Mutations in *TRAPPC11* and knockdown of the protein by RNA interference were shown to have membrane trafficking defects (Milev et al., 2019; Scrivens et al., 2011). I therefore investigated the B18 fibroblasts for defects in membrane trafficking. Here, I used the RUSH

assay (Boncompain et al., 2012) to study the fibroblasts. In the RUSH assay, a fluorescent cargo protein (Sialyl transferase (ST)-eGFP) is retained in the ER until the cells are exposed to biotin. The fluorescent cargo protein is observed as it exits the ER and arrives at the Golgi (Boncompain et al., 2012; Milev et al., 2019). During the assay, there should be an increase in the fluorescence intensity over time as the marker protein arrives at the Golgi. This was seen for control fibroblasts following biotin administration (Figure 3.4A,B). In contrast, the level of fluorescence intensity in the Golgi was significantly less in B18 than in the control. After treatment with Ataluren, the Golgi fluorescence intensity was rescued to levels of intensity approaching that of control. From this finding, I conclude that Ataluren can rescue the ER-to-Golgi trafficking defect in B18 cells.

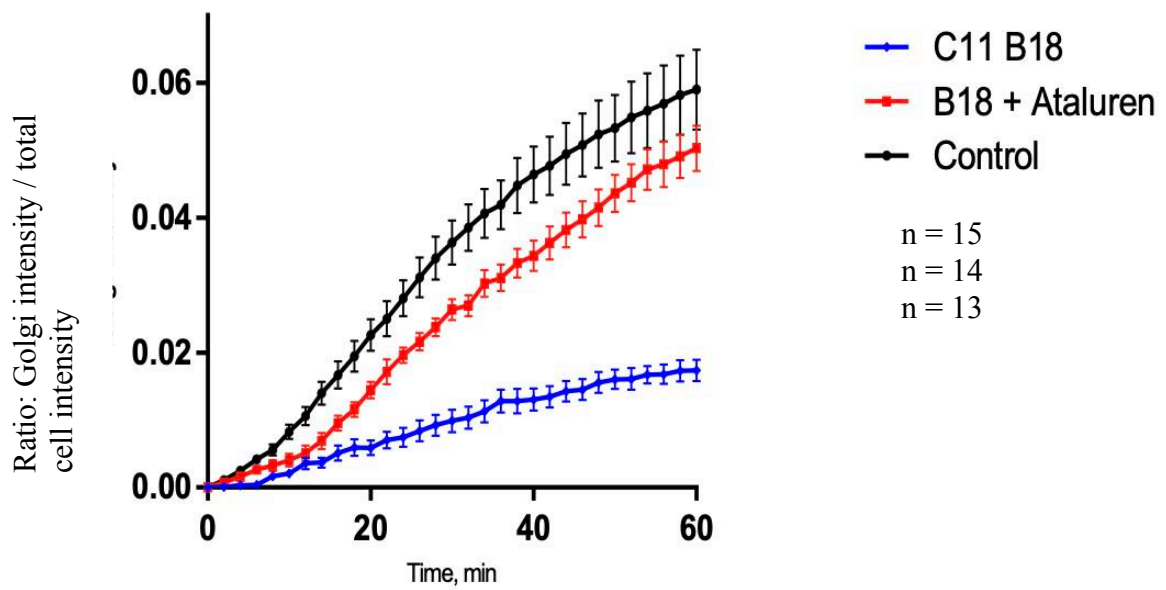
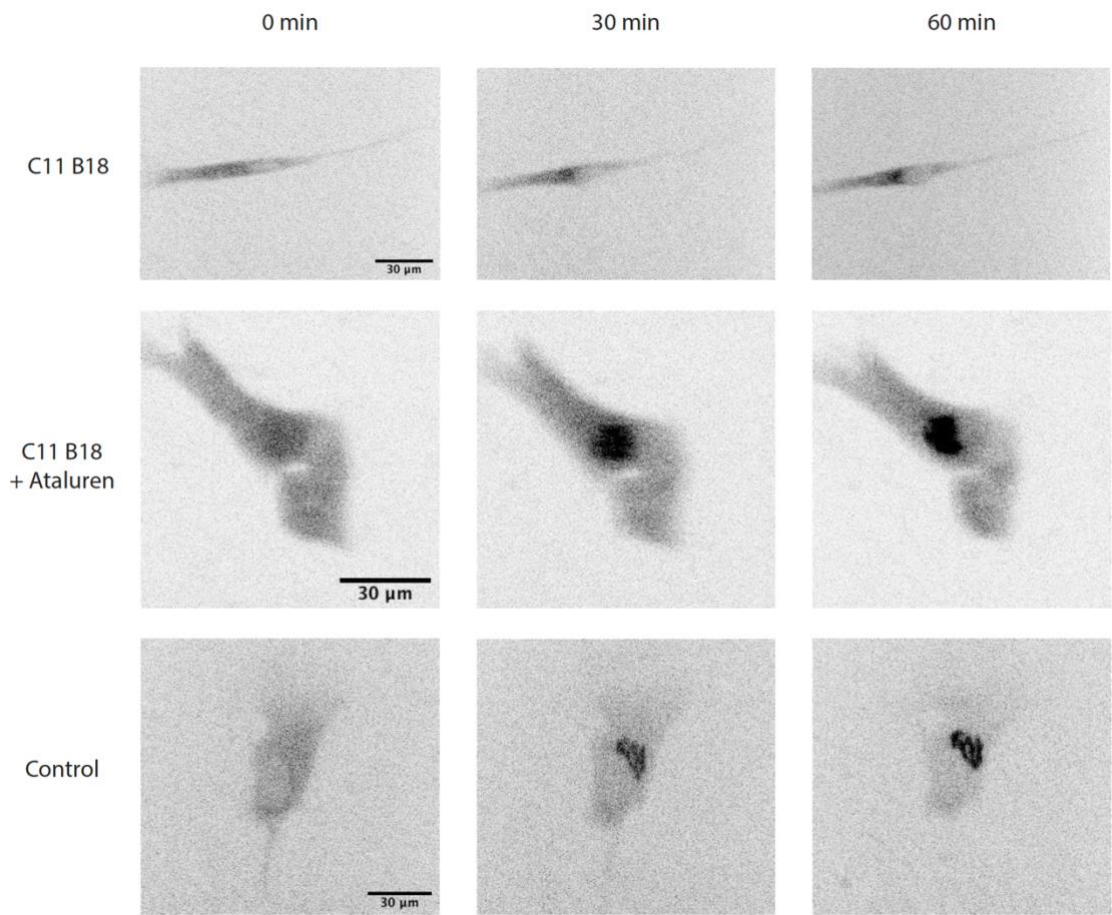


Figure 3.4. Trafficking from ER to the Golgi is defective in B18 fibroblasts and rescued after treatment with Ataluren. The RUSH assay was performed on control and B18 fibroblasts using ST-eGFP. The cells were imaged every 2 minutes over a period of 60 minutes after the addition of biotin, which induced the release of cargo from the ER. Fluorescence in the Golgi was quantified using ImageJ as described in Koehler et al., 2017. Representative images for the time points indicated for each condition are shown above the graph.

3.7 TRIDs do not induce observable read-through in transfected HeLa cells

TRAPPC11 is a difficult protein to analyze in fibroblasts because there is not an efficient antibody to properly study endogenous TRAPPC11 via western blotting. Therefore, different approaches needed to be taken in order to determine if read-through of the nonsense mutation in B18 cells is taking place.

An alternative method was devised using a DNA construct. I created a TRAPPC11 reporter construct containing the entire TRAPPC11 protein to analyze the read-through efficiency of Ataluren and Amlexanox on the nonsense mutation 2407C>T. The nonsense mutation was introduced into the TRAPPC11 reporter construct via site directed mutagenesis. The reporter construct was flanked with an HA-tag at the amino-terminus and a myc-tag at the carboxy-terminus. This should allow for easy visualization of read-through occurring by probing for anti-HA and/or anti-myc via western blotting. A wild-type TRAPPC11 band should appear at 130kDa and the mutant TRAPPC11 band should appear at 88kDa. I evaluated the translational read-through of the 2407C>T nonsense mutation by Ataluren and Amlexanox in transfected HeLa cells by western blotting. First, the HeLa cells were transfected with the reporter constructs. The cells transfected with the mutant construct were either left untreated or treated with Ataluren or Amlexanox 5h after transfection and left for 48h. Western blotting showed a band at 130kDa in the cells transfected with the wild-type construct which indicated full-length TRAPPC11 protein

was produced. In the cells transfected with the mutant construct that were left untreated, there is a polypeptide near 88kDa, which is the expected size of the truncated TRAPPC11 protein. There does not appear to be any obvious read-through after treatment with Ataluren or Amlexanox. I expected there to be two bands in these two lanes: one band at 88kDa and one band at 130kDa. Therefore, there is no indication that Ataluren or Amlexanox are initiating read-through of the nonsense mutation in reporter construct-transfected HeLa cells.

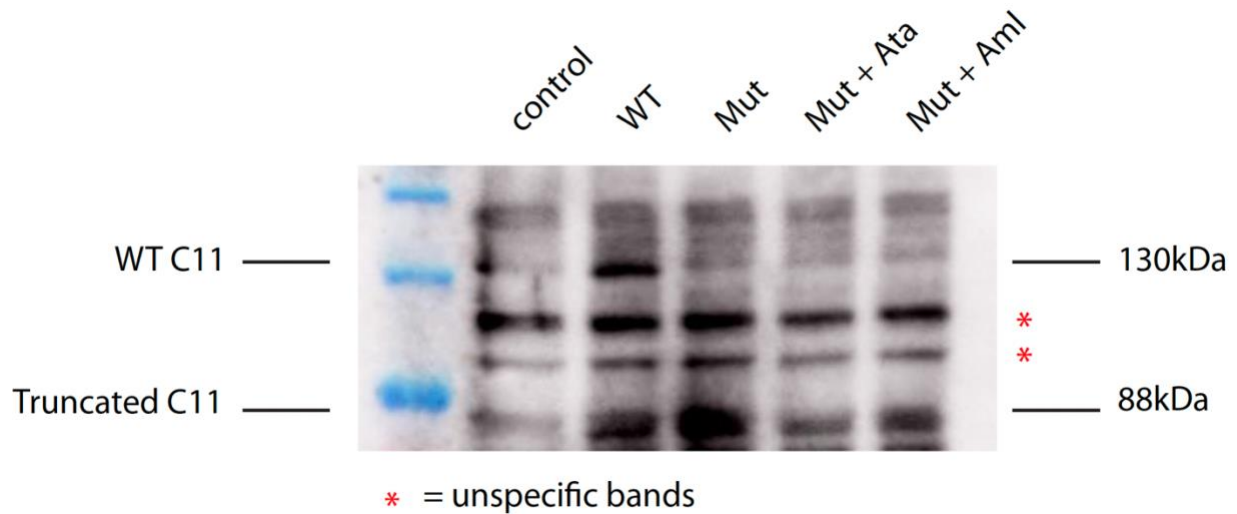


Figure 3.5. HeLa cells transfected with TRAPPC11 reporter construct do not appear to show TRID-induced read-through of the nonsense codon. HeLa cells were either untransfected (control), transfected with the wild-type TRAPPC11 construct (WT), or transfected with TRAPPC11 harboring the c.2407C>T mutation (Mut). The latter transfected cells were left untreated (Mut) or treated with either Ataluren (Mut + Ata) or Amlexanox (Mut + Aml). Lysates were then analyzed by western analysis using anti-HA antibody

4. DISCUSSION

Here, I characterized cellular defects in two different individuals with *TRAPPC11* mutations and studied the efficacy of TRIDs on a nonsense mutation near the gryzun domain of the TRAPPC11 protein. I showed that B18 had cellular defects in autophagy, Golgi morphology and membrane trafficking. In contrast, B19 did not appear to have a defect in autophagy. Instead, the fibroblasts exhibited a similar pattern to the control. However, B19 did show alterations in Golgi morphology. Additionally, I showed that two TRIDs, Ataluren and Amlexanox, rescued the observed cellular defects in B18. These findings suggest that Ataluren and Amlexanox have nonsense mutation read-through properties and can have therapeutic benefits for this allele.

Autophagy was studied here by using a starvation assay to look at the level of LC3-II protein. As seen in figure 3.2, untreated B18 and B19 fibroblasts exhibit clear differences in the levels of LC3-II protein over the course of starvation. B18 fibroblasts showed a very clear defect in autophagy, whereas B19 fibroblasts did not. It has been suggested that the carboxy terminus of the TRAPPC11 protein is critical for proper autophagic function (Milev et al., 2019), How might this explain the differences seen in Figure 3? Recall that both B18 and B19 have the same foie gras deletion variant. In addition to this allele, B18 has a nonsense mutation near the C-terminus, but B19 has a frameshift well before the foie gras domain. It is possible that in B19, the severely-truncated TRAPPC11 protein encoded by this second allele is degraded. This would mean that in this patient, the only functioning TRAPPC11 protein is from the allele with the foie gras mutation which contains the C-terminus required for autophagy. In comparison, the second B18 allele results in a much larger protein that could possibly incorporate into TRAPP III. In such a scenario, a missing C-terminus would be expected to affect autophagy. The difference in

autophagic function seen in individuals with different mutations was also discussed in Milev et al. 2019. There, the authors also found that two subjects with mutations near the C-terminus of the protein had autophagic defects, whereas subjects without C-terminal mutations did not show any autophagic defects.

While starvation experiments are an effective way to observe if there is a rescue in autophagic defect after treatment with TRIDs, there are other methods that can be used to study autophagy that are more specific to TRAPPC11. Within the context of this study, the primary area of focus was the ability for TRIDs to suppress a nonsense mutation and therefore rescue a cellular defect. To take this further and observe the degree of rescued TRAPPC11 protein function, a more specific assay for TRAPPC11 should take place. For example, Stanga et al., 2019, implemented a protease protection assay to study the function of TRAPPC11 in the sealing of isolation membranes. This type of assay would be more effective to show that a specific function of TRAPPC11 (sealing of isolation membranes) is restored after treatment with TRIDs. This would help in proving wild-type protein function is rescued after treatment and augment the argument that Ataluren and Amlexanox can be therapeutically beneficial to individuals with nonsense mutations, especially within *TRAPPC11*.

After identifying a defect and rescue within the autophagic pathway, alterations in Golgi morphology were investigated. Treatment with TRIDs significantly decreased the number of Golgi fragments observed in each B18 cell, suggesting read-through of a nonsense mutation. Here, the term Golgi “fragmentation” was used to describe the alterations seen in Golgi morphology. However, it has been suggested that this term should be used less loosely, and that

more depth should be attained to study changes in Golgi morphology (Makhoul et al., 2019). These investigators state that the structural differences in Golgi morphology can be attributed to the cellular pathway that is disrupted, and it is important to understand the exact type of Golgi fragmentation taking place. Four different types of Golgi fragmentation were proposed: 1) conversion of Golgi ribbon to Golgi stacks, 2) loss of both Golgi ribbon and integrity of Golgi stacks, 3) dispersal of one Golgi compartment, and 4) conversion of the Golgi ribbon to tubulovesicular elements (Figure 4.1). In the fibroblasts studied here, we used Man-II to stain the cis-Golgi ribbon. With the results obtained here, and the four types of Golgi fragmentation proposed, it is possible that the TRAPPC11-induced Golgi fragmentation would be better described as conversion of the Golgi ribbon to tubulovesicular elements (Figure 4.1). To further study the Golgi fragmentation observed, alternate protein antibodies should be used, or different methods of observation should be employed, such as high-resolution optical microscopy or electron microscopy.

Despite the discrepancies in Golgi fragmentation terminology, here we observed an apparent rescue in Golgi morphology. It would be beneficial to utilize different microscopy techniques to observe the rescued Golgi morphology. Regardless of the type of Golgi fragmentation observed in the B18 and B19 cells, I observed that Ataluren and Amlexanox rescued Golgi morphology in patient fibroblasts.

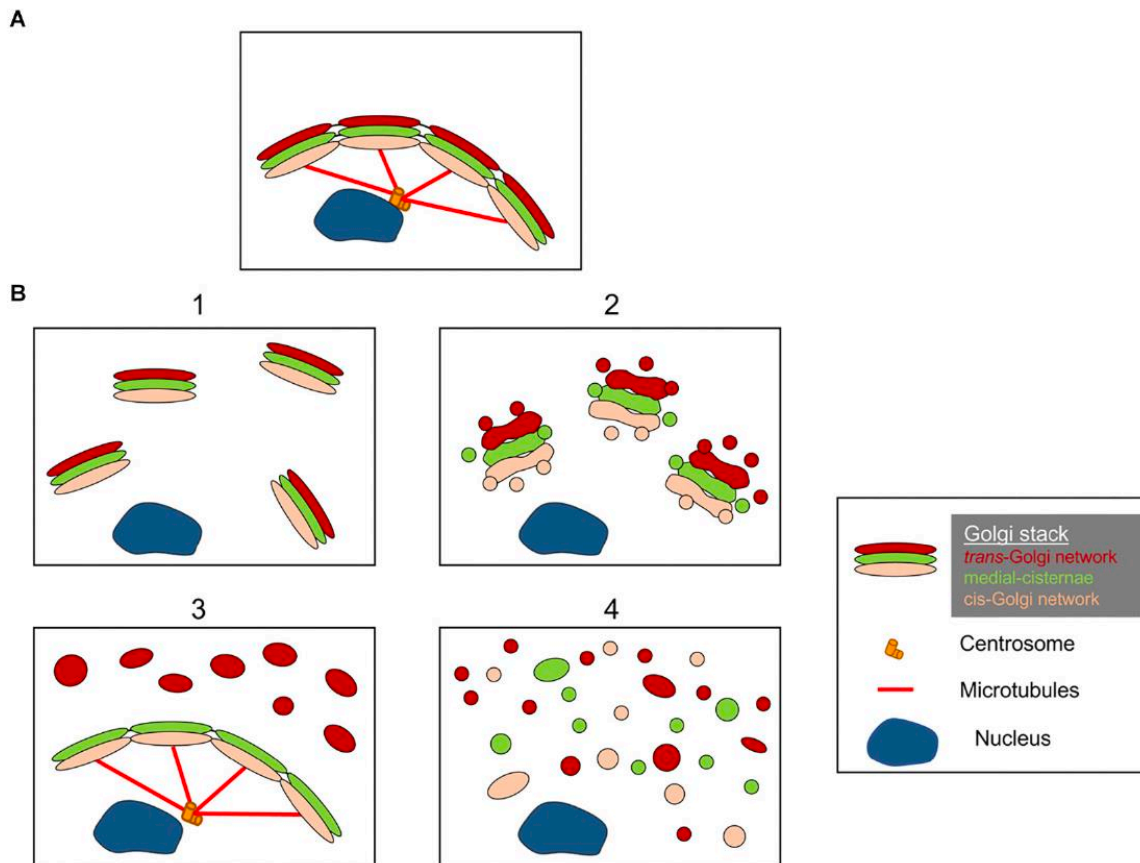


Figure 4.1. Four models of Golgi fragmentation. A) A cartoon of an intact Golgi ribbon structure. B) Four types of fragmentation were proposed by Makhoul et al, 2019. 1. Golgi mini stacks are dispersed throughout the cytoplasm. These ministacks are composed of all three (cis, medial, trans) Golgi subcompartments. 2. Golgi ribbon integrity is compromised with shortened cisternae. 3. Dispersal of one Golgi subcompartment with the other subcompartments remaining intact. 4. Loss of Golgi ribbon and stacks with all subcompartments dispersed as tubules and vesicles. Reproduced from Makhoul et al., 2019.

In addition to autophagy and Golgi morphology, membrane trafficking was investigated. Here, the untreated B18 fibroblasts showed weaker Golgi fluorescence intensity over time compared to the control. In this case, it appears that the trafficking process is delayed and there are less vesicles transporting cargo. This seems apparent due to the fact that at the end of the 60 minute movie, the maximum intensity that the Golgi achieves is significantly less than the control. In this case, further study into TRAPPC11 and its role in vesicle trafficking needs to be done. The

results found with B18 and Ataluren are preliminary, as Amlexanox has not been tested yet and the RUSH assay for B19 was inconclusive. It was unclear in the case of B19 if the membrane trafficking defect is a complete blockage of protein movement from the ER to the Golgi, or if there was an error in the assay. The RUSH assay needs to be repeated with Amlexanox and for B19. Regardless, the capability of Ataluren to suppress the c.2407C>T nonsense mutation was observed.

Having visual confirmation that read-through is taking place would more conclusively demonstrate that the drugs were indeed acting via read-through of the nonsense codon. Here, transfected HeLa cells were used to determine if read-through occurs since our TRAPPC11 antibody is not ideal to visualize TRAPPC11. This experiment was performed in HeLa cells because they can be transfected easily, have fast cell growth, and are stable enough to tolerate transfection and subsequent drug treatment. HeLa cells should also express the HA and/or myc tags clearly. However, I was unable to successfully detect read-through of the construct. It is possible that within HeLa cells, the mechanism of read-through is different from fibroblasts. This assay completed here was modeled after the reporter construct assay conducted in Samanta et al., 2019, and in their study, they used HEK293T transfected cells and were able to detect read-through. Ideally, this assay should be conducted in fibroblasts to provide consistency throughout all experiments. In the future, this assay could be redone by transfecting fibroblasts with the reporter construct and observing read-through via western blotting.

It is peculiar that there is no read-through observed in the transfected HeLa cells, but the rescue of various cellular processes was observed in fibroblasts. It has been suggested that less than 1%

of read-through can, in some cases, be therapeutically beneficial (Gunn et al., 2014; Schilff et al., 2021). This might account for the rescue seen in defective autophagy, Golgi morphology and membrane trafficking pathways. It is important to note that the level of read-through necessary to restore cellular function varies greatly between diseases, so what is considered therapeutic in one disease might not be the case for another (Schilff et al., 2021).

Throughout this work, I treated cells with either Ataluren or Amlexanox, but never both. It has been suggested that treating cells with an NMD inhibitor along with a read-through inducing drug there could be more efficient read-through (Eintracht et al., 2021; Gonzalez-Hilarion et al., 2012). In theory, inhibiting NMD would prevent the cell from degrading mutant mRNA transcripts, thus providing more stable transcripts for a read-through inducing drug to act upon. Additionally, one study showed that using a small molecule compound that does not stimulate read-through on its own, in addition to a TRID, the read-through of a nonsense mutation might be enhanced (Hosseini-Farahabadi et al., 2021). Future work could include using two drugs, or a small molecule enhancer (such as γ -320, seen in (Hosseini-Farahabadi et al., 2021)), in addition to a TRID and observing whether there is even more improvement in the already seen rescue of cellular defects.

Treatment of nonsense mutation-mediated diseases deserves more recognition and aggressive study. As mentioned, nearly 12% of all human genetic diseases are attributed to nonsense mutations (Ng et al., 2021). On one hand, this work could be applied to treat nonsense mutations in different TRAPP proteins. After observing the rescue of cellular defects in the TRAPPC11 patients presented here, a member of the Sacher lab is currently examining the effect of Ataluren

on a nonsense mutation in a TRAPPC6B mutant individual. Positive results have been observed thus far, proving promising potential for the read-through of other TRAPP-related mutations. On the other hand, this work can be used to enhance the argument behind the therapeutic potential of Ataluren and Amlexanox, as both drugs have shown their capabilities of rescuing cellular defects here. Amlexanox needs to be studied more thoroughly and needs to be used to treat other nonsense mutations, such as the TRAPPC6B mutation mentioned earlier. Ataluren needs to be fine-tuned and possibly used with the addition of a small molecule compound to enhance its read-through properties. In all, treating nonsense mutations can aid in the treatment of various diseases, potentially alleviate detrimental side effects, and ultimately change the lives of thousands of individuals.

Citations

- Antonescu, C. N., McGraw, T. E., & Klip, A. (2014). Reciprocal Regulation of Endocytosis and Metabolism. *Cold Spring Harbor Perspectives in Biology*, 6(7), a016964–a016964. <https://doi.org/10.1101/cshperspect.a016964>
- Atanasova, V. S., Jiang, Q., Prisco, M., Gruber, C., Piñón Hofbauer, J., Chen, M., Has, C., Bruckner-Tuderman, L., McGrath, J. A., Uitto, J., & South, A. P. (2017). Amlexanox Enhances Premature Termination Codon Read-Through in COL7A1 and Expression of Full Length Type VII Collagen: Potential Therapy for Recessive Dystrophic Epidermolysis Bullosa. *Journal of Investigative Dermatology*, 137(9), 1842–1849. <https://doi.org/10.1016/j.jid.2017.05.011>
- Barlowe, C. (1994). COPII: A membrane coat formed by Sec proteins that drive vesicle budding from the endoplasmic reticulum. *Cell*, 77(6), 895–907. [https://doi.org/10.1016/0092-8674\(94\)90138-4](https://doi.org/10.1016/0092-8674(94)90138-4)
- Bassik, M. C., Kampmann, M., Lebbink, R. J., Wang, S., Hein, M. Y., Poser, I., Weibezahn, J., Horlbeck, M. A., Chen, S., Mann, M., Hyman, A. A., LeProust, E. M., McManus, M. T., & Weissman, J. S. (2013). A Systematic Mammalian Genetic Interaction Map Reveals Pathways Underlying Ricin Susceptibility. *Cell*, 152(4), 909–922. <https://doi.org/10.1016/j.cell.2013.01.030>
- Behrends, C., Sowa, M. E., Gygi, S. P., & Harper, J. W. (2010). Network organization of the human autophagy system. *Nature*, 466(7302), 68–76. <https://doi.org/10.1038/nature09204>

- Bi, X., Corpina, R. A., & Goldberg, J. (2002). Structure of the Sec23/24–Sar1 pre-budding complex of the COPII vesicle coat. *Nature*, *419*(6904), 271–277.
<https://doi.org/10.1038/nature01040>
- Bidou, L., Hatin, I., Perez, N., Allamand, V., Panthier, J.-J., & Rousset, J.-P. (2004). Premature stop codons involved in muscular dystrophies show a broad spectrum of readthrough efficiencies in response to gentamicin treatment. *Gene Therapy*, *11*(7), 619–627.
<https://doi.org/10.1038/sj.gt.3302211>
- Blomen, V. A., Májek, P., Jae, L. T., Bigenzahn, J. W., Nieuwenhuis, J., Staring, J., Sacco, R., van Diemen, F. R., Olk, N., Stukalov, A., Marceau, C., Janssen, H., Carette, J. E., Bennett, K. L., Colinge, J., Superti-Furga, G., & Brummelkamp, T. R. (2015). Gene essentiality and synthetic lethality in haploid human cells. *Science*, *350*(6264), 1092–1096. <https://doi.org/10.1126/science.aac7557>
- Bögershausen, N., Shahrzad, N., Chong, J. X., von Kleist-Retzow, J.-C., Stanga, D., Li, Y., Bernier, F. P., Loucks, C. M., Wirth, R., Puffenberger, E. G., Hegele, R. A., Schreml, J., Lapointe, G., Keupp, K., Brett, C. L., Anderson, R., Hahn, A., Innes, A. M., Suchowersky, O., ... Lamont, R. E. (2013). Recessive TRAPPC11 Mutations Cause a Disease Spectrum of Limb Girdle Muscular Dystrophy and Myopathy with Movement Disorder and Intellectual Disability. *The American Journal of Human Genetics*, *93*(1), 181–190. <https://doi.org/10.1016/j.ajhg.2013.05.028>
- Boncompain, G., Divoux, S., Gareil, N., de Forges, H., Lescure, A., Latreche, L., Mercanti, V., Jollivet, F., Raposo, G., & Perez, F. (2012). Synchronization of secretory protein traffic in populations of cells. *Nature Methods*, *9*(5), 493–498.
<https://doi.org/10.1038/nmeth.1928>

- Bonifacino, J. S., & Glick, B. S. (2004). The Mechanisms of Vesicle Budding and Fusion. *Cell*, *116*(2), 153–166. [https://doi.org/10.1016/S0092-8674\(03\)01079-1](https://doi.org/10.1016/S0092-8674(03)01079-1)
- Bonifacino, J. S., & Lippincott-Schwartz, J. (2003). Coat proteins: Shaping membrane transport. *Nature Reviews Molecular Cell Biology*, *4*(5), 409–414. <https://doi.org/10.1038/nrm1099>
- Boya, P., Reggiori, F., & Codogno, P. (2013). Emerging regulation and functions of autophagy. *Nature Cell Biology*, *15*(7), 713–720. <https://doi.org/10.1038/ncb2788>
- Bröcker, C., Engelbrecht-Vandré, S., & Ungermann, C. (2010). Multisubunit Tethering Complexes and Their Role in Membrane Fusion. *Current Biology*, *20*(21), R943–R952. <https://doi.org/10.1016/j.cub.2010.09.015>
- Brunet, S., Noueihed, B., Shahrzad, N., Saint-Dic, D., Hasaj, B., Guan, T. L., Moores, A., Barlowe, C., & Sacher, M. (2012). The SMS domain of Trs23p is responsible for the in vitro appearance of the TRAPP I complex in *Saccharomyces cerevisiae*. *Cellular Logistics*, *2*(1), 28–42. <https://doi.org/10.4161/cl.19414>
- Brunet, S., Shahrzad, N., Saint-Dic, D., Dutczak, H., & Sacher, M. (2013). A *trs20* Mutation That Mimics an SEDT-Causing Mutation Blocks Selective and Non-Selective Autophagy: A Model for TRAPP III Organization: *trs20D46Y* Affects Autophagy. *Traffic*, *14*(10), 1091–1104. <https://doi.org/10.1111/tra.12095>
- Cai, Y., Chin, H. F., Lazarova, D., Menon, S., Fu, C., Cai, H., Sclafani, A., Rodgers, D. W., De La Cruz, E. M., Ferro-Novick, S., & Reinisch, K. M. (2008). The Structural Basis for Activation of the Rab Ypt1p by the TRAPP Membrane-Tethering Complexes. *Cell*, *133*(7), 1202–1213. <https://doi.org/10.1016/j.cell.2008.04.049>
- DeRossi, C., Vacaru, A., Rafiq, R., Cinaroglu, A., Imrie, D., Nayar, S., Baryshnikova, A., Milev, M. P., Stanga, D., Kadakia, D., Gao, N., Chu, J., Freeze, H. H., Lehrman, M. A., Sacher,

- M., & Sadler, K. C. (2016). *Trappc11* is required for protein glycosylation in zebrafish and humans. *Molecular Biology of the Cell*, 27(8), 1220–1234.
<https://doi.org/10.1091/mbc.E15-08-0557>
- Eintracht, J., Forsythe, E., May-Simera, H., & Moosajee, M. (2021). Translational readthrough of ciliopathy genes BBS2 and ALMS1 restores protein, ciliogenesis and function in patient fibroblasts. *EBioMedicine*, 70, 103515.
<https://doi.org/10.1016/j.ebiom.2021.103515>
- Eskelinen, E.-L. (2005). Maturation of Autophagic Vacuoles in Mammalian Cells. *Autophagy*, 1(1), 1–10. <https://doi.org/10.4161/auto.1.1.1270>
- Fasshauer, D., Eliason, W. K., Brünger, A. T., & Jahn, R. (1998). Identification of a Minimal Core of the Synaptic SNARE Complex Sufficient for Reversible Assembly and Disassembly. *Biochemistry*, 37(29), 10354–10362. <https://doi.org/10.1021/bi980542h>
- Fee, D. B., Harmelink, M., Monrad, P., & Pyzik, E. (2017). Siblings With Mutations in TRAPPC11 Presenting With Limb-Girdle Muscular Dystrophy 2S. *Journal of Clinical Neuromuscular Disease*, 19(1), 27–30. <https://doi.org/10.1097/CND.000000000000173>
- Galindo, A., Planelles-Herrero, V. J., Degliesposti, G., & Munro, S. (2021). Cryo-EM structure of metazoan TRAPPIII, the multi-subunit complex that activates the GTPase Rab1. *The EMBO Journal*, 40(12). <https://doi.org/10.15252/embj.2020107608>
- Gonzalez-Hilarion, S., Beghyn, T., Jia, J., Debreuck, N., Berte, G., Mamchaoui, K., Mouly, V., Gruenert, D. C., Déprez, B., & Lejeune, F. (2012). Rescue of nonsense mutations by amlexanox in human cells. *Orphanet Journal of Rare Diseases*, 7(1), 58.
<https://doi.org/10.1186/1750-1172-7-58>

- Gunn, G., Dai, Y., Du, M., Belakhov, V., Kandasamy, J., Schoeb, T. R., Baasov, T., Bedwell, D. M., & Keeling, K. M. (2014). Long-term nonsense suppression therapy moderates MPS I-H disease progression. *Molecular Genetics and Metabolism*, *111*(3), 374–381. <https://doi.org/10.1016/j.ymgme.2013.12.007>
- Hart, T., Chandrashekhar, M., Aregger, M., Steinhart, Z., Brown, K. R., MacLeod, G., Mis, M., Zimmermann, M., Fradet-Turcotte, A., Sun, S., Mero, P., Dirks, P., Sidhu, S., Roth, F. P., Rissland, O. S., Durocher, D., Angers, S., & Moffat, J. (2015). High-Resolution CRISPR Screens Reveal Fitness Genes and Genotype-Specific Cancer Liabilities. *Cell*, *163*(6), 1515–1526. <https://doi.org/10.1016/j.cell.2015.11.015>
- Hosseini-Farahabadi, S., Baradaran-Heravi, A., Zimmerman, C., Choi, K., Flibotte, S., & Roberge, M. (2021). Small molecule Y-320 stimulates ribosome biogenesis, protein synthesis, and aminoglycoside-induced premature termination codon readthrough. *PLOS Biology*, *19*(5), e3001221. <https://doi.org/10.1371/journal.pbio.3001221>
- Howell, G. J., Holloway, Z. G., Cobbold, C., Monaco, A. P., & Ponnambalam, S. (2006). Cell Biology of Membrane Trafficking in Human Disease. In *International Review of Cytology* (Vol. 252, pp. 1–69). Elsevier. [https://doi.org/10.1016/S0074-7696\(06\)52005-4](https://doi.org/10.1016/S0074-7696(06)52005-4)
- Joiner, A. M., Phillips, B. P., Yugandhar, K., Sanford, E. J., Smolka, M. B., Yu, H., Miller, E. A., & Fromme, J. C. (2021). Structural basis of TRAPPIII-mediated Rab1 activation. *The EMBO Journal*, *40*(12). <https://doi.org/10.15252/emboj.2020107607>
- Kabeya, Y. (2000). LC3, a mammalian homologue of yeast Apg8p, is localized in autophagosome membranes after processing. *The EMBO Journal*, *19*(21), 5720–5728. <https://doi.org/10.1093/emboj/19.21.5720>

- Kim, J. J., Lipatova, Z., & Segev, N. (2016). TRAPP Complexes in Secretion and Autophagy. *Frontiers in Cell and Developmental Biology*, 4. <https://doi.org/10.3389/fcell.2016.00020>
- Kishi-Itakura, C., Koyama-Honda, I., Itakura, E., & Mizushima, N. (2014). Ultrastructural analysis of autophagosome organization using mammalian autophagy-deficient cells. *Journal of Cell Science*, jcs.156034. <https://doi.org/10.1242/jcs.156034>
- Klann, M., Koepl, H., & Reuss, M. (2012). Spatial Modeling of Vesicle Transport and the Cytoskeleton: The Challenge of Hitting the Right Road. *PLoS ONE*, 7(1), e29645. <https://doi.org/10.1371/journal.pone.0029645>
- Klionsky, D. J., Abdel-Aziz, A. K., Abdelfatah, S., Abdellatif, M., Abdoli, A., Abel, S., Abeliovich, H., Abildgaard, M. H., Abudu, Y. P., Acevedo-Arozena, A., Adamopoulos, I. E., Adeli, K., Adolph, T. E., Adornetto, A., Aflaki, E., Agam, G., Agarwal, A., Aggarwal, B. B., Agnello, M., ... Tong, C.-K. (2021). Guidelines for the use and interpretation of assays for monitoring autophagy (4th edition) ¹. *Autophagy*, 17(1), 1–382. <https://doi.org/10.1080/15548627.2020.1797280>
- Koehler, K., Milev, M. P., Prematilake, K., Reschke, F., Kutzner, S., Jühlen, R., Landgraf, D., Utine, E., Hazan, F., Diniz, G., Schuelke, M., Huebner, A., & Sacher, M. (2017). A novel *TRAPPC11* mutation in two Turkish families associated with cerebral atrophy, global retardation, scoliosis, achalasia and alacrima. *Journal of Medical Genetics*, 54(3), 176–185. <https://doi.org/10.1136/jmedgenet-2016-104108>
- Larson, A. A., Baker, P. R., Milev, M. P., Press, C. A., Sokol, R. J., Cox, M. O., Lekostaj, J. K., Stence, A. A., Bossler, A. D., Mueller, J. M., Prematilake, K., Tadjó, T. F., Williams, C. A., Sacher, M., & Moore, S. A. (2018). TRAPPC11 and GOSR2 mutations associate with

- hypoglycosylation of α -dystroglycan and muscular dystrophy. *Skeletal Muscle*, 8(1), 17.
<https://doi.org/10.1186/s13395-018-0163-0>
- Lejeune, F. (2017). Nonsense-mediated mRNA decay at the crossroads of many cellular pathways. *BMB Reports*, 50(4), 175–185.
<https://doi.org/10.5483/BMBRep.2017.50.4.015>
- Letourneur, F., Gaynor, E. C., Hennecke, S., Démollière, C., Duden, R., Emr, S. D., Riezman, H., & Cosson, P. (1994). Coatamer is essential for retrieval of dilysine-tagged proteins to the endoplasmic reticulum. *Cell*, 79(7), 1199–1207. [https://doi.org/10.1016/0092-8674\(94\)90011-6](https://doi.org/10.1016/0092-8674(94)90011-6)
- Liang, W.-C., Zhu, W., Mitsuhashi, S., Noguchi, S., Sacher, M., Ogawa, M., Shih, H.-H., Jong, Y.-J., & Nishino, I. (2015). Congenital muscular dystrophy with fatty liver and infantile-onset cataract caused by TRAPPC11 mutations: Broadening of the phenotype. *Skeletal Muscle*, 5(1), 29. <https://doi.org/10.1186/s13395-015-0056-4>
- Makhoul, C., Gosavi, P., & Gleeson, P. A. (2019). Golgi Dynamics: The Morphology of the Mammalian Golgi Apparatus in Health and Disease. *Frontiers in Cell and Developmental Biology*, 7, 112. <https://doi.org/10.3389/fcell.2019.00112>
- Maquat, L. E. (2004). Nonsense-mediated mRNA decay: Splicing, translation and mRNP dynamics. *Nature Reviews Molecular Cell Biology*, 5(2), 89–99.
<https://doi.org/10.1038/nrm1310>
- Matalonga, L., Bravo, M., Serra-Peinado, C., García-Pelegri, E., Ugarteburu, O., Vidal, S., Llambrich, M., Quintana, E., Fuster-Jorge, P., Gonzalez-Bravo, M. N., Beltran, S., Dopazo, J., Garcia-Garcia, F., Foulquier, F., Matthijs, G., Mills, P., Ribes, A., Egea, G., Briones, P., ... Girós, M. (2017). Mutations in *TRAPPC11* are associated with a

- congenital disorder of glycosylation: HUMAN MUTATION. *Human Mutation*, 38(2), 148–151. <https://doi.org/10.1002/humu.23145>
- Michorowska, S. (2021). Ataluren—Promising Therapeutic Premature Termination Codon Readthrough Frontrunner. *Pharmaceuticals*, 14(8), 785. <https://doi.org/10.3390/ph14080785>
- Milev, M. P., Stanga, D., Schänzer, A., Nascimento, A., Saint-Dic, D., Ortez, C., Natera-de Benito, D., Barrios, D. G., Colomer, J., Badosa, C., Jou, C., Gallano, P., Gonzalez-Quereda, L., Töpf, A., Johnson, K., Straub, V., Hahn, A., Sacher, M., & Jimenez-Mallebrera, C. (2019). Characterization of three TRAPPC11 variants suggests a critical role for the extreme carboxy terminus of the protein. *Scientific Reports*, 9(1), 14036. <https://doi.org/10.1038/s41598-019-50415-6>
- Munot, P., McCrea, N., Torelli, S., Manzur, A., Sewry, C., Chambers, D., Feng, L., Ala, P., Zaharieva, I., Ragge, N., Roper, H., Marton, T., Cox, P., Milev, M. P., Liang, W., Maruyama, S., Nishino, I., Sacher, M., Phadke, R., & Muntoni, F. (2022). *TRAPPC11* - related muscular dystrophy with hypoglycosylation of alpha-dystroglycan in skeletal muscle and brain. *Neuropathology and Applied Neurobiology*, 48(2). <https://doi.org/10.1111/nan.12771>
- Nagel-Wolfrum, K., Möller, F., Penner, I., Baasov, T., & Wolfrum, U. (2016). Targeting Nonsense Mutations in Diseases with Translational Read-Through-Inducing Drugs (TRIDs). *BioDrugs*, 30(2), 49–74. <https://doi.org/10.1007/s40259-016-0157-6>
- Ng, M. Y., Li, H., Ghelfi, M. D., Goldman, Y. E., & Cooperman, B. S. (2021). Ataluren and aminoglycosides stimulate read-through of nonsense codons by orthogonal mechanisms.

- Proceedings of the National Academy of Sciences*, 118(2), e2020599118.
<https://doi.org/10.1073/pnas.2020599118>
- Nichols, B. J., Ungermann, C., Pelham, H. R. B., Wickner, W. T., & Haas, A. (1997). Homotypic vacuolar fusion mediated by t- and v-SNAREs. *Nature*, 387(6629), 199–202.
<https://doi.org/10.1038/387199a0>
- Palade, G. (1975). Intracellular Aspects of the Process of Protein Synthesis. *Science*, 189(4200), 347–358. <https://doi.org/10.1126/science.1096303>
- Pearse, B. M. (1976). Clathrin: A unique protein associated with intracellular transfer of membrane by coated vesicles. *Proceedings of the National Academy of Sciences*, 73(4), 1255–1259. <https://doi.org/10.1073/pnas.73.4.1255>
- Peltz, S. W., Morsy, M., Welch, E. M., & Jacobson, A. (2013). Ataluren as an Agent for Therapeutic Nonsense Suppression. *Annual Review of Medicine*, 64(1), 407–425.
<https://doi.org/10.1146/annurev-med-120611-144851>
- Rossi, G., Kolstad, K., Stone, S., Palluault, F., & Ferro-Novick, S. (1995). BET3 encodes a novel hydrophilic protein that acts in conjunction with yeast SNAREs. *Molecular Biology of the Cell*, 6(12), 1769–1780. <https://doi.org/10.1091/mbc.6.12.1769>
- Rubinsztein, D. C., Shpilka, T., & Elazar, Z. (2012). Mechanisms of Autophagosome Biogenesis. *Current Biology*, 22(1), R29–R34. <https://doi.org/10.1016/j.cub.2011.11.034>
- Sacher, M. (1998). TRAPP, a highly conserved novel complex on the cis-Golgi that mediates vesicle docking and fusion. *The EMBO Journal*, 17(9), 2494–2503.
<https://doi.org/10.1093/emboj/17.9.2494>

- Sacher, M., Barrowman, J., Schieltz, D., Yates, J. R., & Ferro-Novick, S. (2000). Identification and characterization of five new subunits of TRAPP. *European Journal of Cell Biology*, 79(2), 71–80. [https://doi.org/10.1078/S0171-9335\(04\)70009-6](https://doi.org/10.1078/S0171-9335(04)70009-6)
- Sacher, M., Shahrzad, N., Kamel, H., & Milev, M. P. (2019). TRAPPopathies: An emerging set of disorders linked to variations in the genes encoding transport protein particle (TRAPP)-associated proteins. *Traffic*, 20(1), 5–26. <https://doi.org/10.1111/tra.12615>
- Sagiv, Y. (2000). GATE-16, a membrane transport modulator, interacts with NSF and the Golgi v-SNARE GOS-28. *The EMBO Journal*, 19(7), 1494–1504. <https://doi.org/10.1093/emboj/19.7.1494>
- Samanta, A., Stingl, K., Kohl, S., Ries, J., Linnert, J., & Nagel-Wolfrum, K. (2019). Ataluren for the Treatment of Usher Syndrome 2A Caused by Nonsense Mutations. *International Journal of Molecular Sciences*, 20(24), 6274. <https://doi.org/10.3390/ijms20246274>
- Schilff, M., Sargsyan, Y., Hofhuis, J., & Thoms, S. (2021). Stop Codon Context-Specific Induction of Translational Readthrough. *Biomolecules*, 11(7), 1006. <https://doi.org/10.3390/biom11071006>
- Scrivens, P. J., Noueihed, B., Shahrzad, N., Hul, S., Brunet, S., & Sacher, M. (2011). C4orf41 and TTC-15 are mammalian TRAPP components with a role at an early stage in ER-to-Golgi trafficking. *Molecular Biology of the Cell*, 22(12), 2083–2093. <https://doi.org/10.1091/mbc.e10-11-0873>
- Stanga, D., Zhao, Q., Milev, M. P., Saint-Dic, D., Jimenez-Mallebrera, C., & Sacher, M. (2019). TRAPPC11 functions in autophagy by recruiting ATG2B-WIPI4/WDR45 to preautophagosomal membranes. *Traffic*, 20(5), 325–345. <https://doi.org/10.1111/tra.12640>

- Stephens, D. J., Lin-Marq, N., Pagano, A., Pepperkok, R., & Paccaud, J. P. (2000). COPI-coated ER-to-Golgi transport complexes segregate from COPII in close proximity to ER exit sites. *Journal of Cell Science*, *113*(12), 2177–2185.
<https://doi.org/10.1242/jcs.113.12.2177>
- Sutton, R. B., Fasshauer, D., Jahn, R., & Brunger, A. T. (1998). Crystal structure of a SNARE complex involved in synaptic exocytosis at 2.4 Å resolution. *Nature*, *395*(6700), 347–353. <https://doi.org/10.1038/26412>
- Tanida, I., Komatsu, M., Ueno, T., & Kominami, E. (2003). GATE-16 and GABARAP are authentic modifiers mediated by Apg7 and Apg3. *Biochemical and Biophysical Research Communications*, *300*(3), 637–644. [https://doi.org/10.1016/S0006-291X\(02\)02907-8](https://doi.org/10.1016/S0006-291X(02)02907-8)
- Thomas, L. L., Joiner, A. M. N., & Fromme, J. C. (2018). The TRAPPIII complex activates the GTPase Ypt1 (Rab1) in the secretory pathway. *Journal of Cell Biology*, *217*(1), 283–298. <https://doi.org/10.1083/jcb.201705214>
- Velikkakath, A. K. G., Nishimura, T., Oita, E., Ishihara, N., & Mizushima, N. (2012). Mammalian Atg2 proteins are essential for autophagosome formation and important for regulation of size and distribution of lipid droplets. *Molecular Biology of the Cell*, *23*(5), 896–909. <https://doi.org/10.1091/mbc.e11-09-0785>
- Vössing, C., Owczarek-Lipska, M., Nagel-Wolfrum, K., Reiff, C., Jüschke, C., & Neidhardt, J. (2020). Translational Read-Through Therapy of RPGR Nonsense Mutations. *International Journal of Molecular Sciences*, *21*(22), 8418. <https://doi.org/10.3390/ijms21228418>

- Wang, T., Birsoy, K., Hughes, N. W., Krupczak, K. M., Post, Y., Wei, J. J., Lander, E. S., & Sabatini, D. M. (2015). Identification and characterization of essential genes in the human genome. *Science*, *350*(6264), 1096–1101. <https://doi.org/10.1126/science.aac7041>
- Welch, E. M., Barton, E. R., Zhuo, J., Tomizawa, Y., Friesen, W. J., Trifillis, P., Paushkin, S., Patel, M., Trotta, C. R., Hwang, S., Wilde, R. G., Karp, G., Takasugi, J., Chen, G., Jones, S., Ren, H., Moon, Y.-C., Corson, D., Turpoff, A. A., ... Sweeney, H. L. (2007). PTC124 targets genetic disorders caused by nonsense mutations. *Nature*, *447*(7140), 87–91. <https://doi.org/10.1038/nature05756>
- Zhao, S., Li, C. M., Luo, X. M., Siu, G. K. Y., Gan, W. J., Zhang, L., Wu, W. K. K., Chan, H. C., & Yu, S. (2017). Mammalian TRAPPIII Complex positively modulates the recruitment of Sec13/31 onto COPII vesicles. *Scientific Reports*, *7*(1), 43207. <https://doi.org/10.1038/srep43207>
- Zheng, J.-X., Li, Y., Ding, Y.-H., Liu, J.-J., Zhang, M.-J., Dong, M.-Q., Wang, H.-W., & Yu, L. (2017). Architecture of the ATG2B-WDR45 complex and an aromatic Y/HF motif crucial for complex formation. *Autophagy*, *13*(11), 1870–1883. <https://doi.org/10.1080/15548627.2017.1359381>